

Hydroxyl radical-involved cancer therapy via Fenton reactions

Mengying Liu¹, Yun Xu², Yanjun Zhao¹, Zheng Wang (✉)¹, Dunyun Shi (✉)³

¹ School of Pharmaceutical Science & Technology, Tianjin University, Tianjin 300072, China

² Central Lab, Shenzhen Second People's Hospital/the First Affiliated Hospital of Shenzhen University, Shenzhen 518035, China

³ Institute of Hematology, Shenzhen Second People's Hospital/the First Affiliated Hospital of Shenzhen University, Shenzhen 518035, China

© Higher Education Press 2021

Abstract The tumor microenvironment features over-expressed hydrogen peroxide (H_2O_2). Thus, versatile therapeutic strategies based on H_2O_2 as a reaction substrate to generate hydroxyl radical ($\bullet OH$) have been used as a prospective therapeutic method to boost anticancer efficiency. However, the limited Fenton catalysts and insufficient endogenous H_2O_2 content in tumor sites greatly hinder $\bullet OH$ production, failing to achieve the desired therapeutic effect. Therefore, supplying Fenton catalysts and elevating H_2O_2 levels into cancer cells are effective strategies to improve $\bullet OH$ generation. These therapeutic strategies are systematically discussed in this review. Furthermore, the challenges and future developments of hydroxyl radical-involved cancer therapy are discussed to improve therapeutic efficacy.

Keywords hydroxyl radical, Fenton catalyst, hydrogen peroxide, cancer therapy

1 Introduction

Currently, the high mortality rate of cancer is a big threat to human health because of its complexity and versatility [1]. In this regard, scientific research on efficient cancer therapy is necessary. Therefore, the development of various effective anticancer agents has become a top priority. In recent years, reactive oxygen species (ROS) [2], including superoxide anion ($O_2^{\bullet -}$) [3], hydrogen peroxide (H_2O_2) [4], hydroxyl radical ($\bullet OH$) [5], and singlet oxygen (1O_2) [6], have been considered as important therapeutic agents for cancer therapy because of their ability to induce cancer apoptosis. The traditional ROS-based therapies, such as photodynamic therapy [7],

radiotherapy [8], and sonodynamic therapy [9], require exogenous energy input to induce cancer cell death, resulting in serious damage to surrounding normal tissues or cells. However, chemodynamic therapy utilizes endogenous chemical reactions between Fenton catalysts and H_2O_2 to produce $\bullet OH$ without external energy input [10]. Therefore, damage on normal cells or tissues can be avoided. The content of H_2O_2 in cancer cells is higher than that in normal cells. The H_2O_2 content in tumor cells is approximately $0.1\text{--}1\text{ mmol}\cdot\text{L}^{-1}$ [11], whereas that in normal cells is nearly $1\text{--}8\text{ }\mu\text{mol}\cdot\text{L}^{-1}$ in a dynamic balance [12,13]. Nevertheless, the $\bullet OH$ generation depends not only on intracellular H_2O_2 content but also on the Fenton catalysts. As a classical Fenton catalyst, iron ions can trigger $\bullet OH$ generation by reacting with over-produced H_2O_2 in tumor cells [14–16]. Free iron ions in cells are low and primarily found in ferritin and hemosiderin proteins [17,18]. Thus, iron-based nanocarriers have been extensively fabricated to transport iron ions into cells, thereby increasing $\bullet OH$ generation [19–22].

Apart from iron-based Fenton catalysts, other metal-based catalysts can be used to generate $\bullet OH$ through Fenton-like reactions, such as Mn-based Fenton catalysts and Cu-based Fenton catalysts. Once internalized by cancer cells, the Fenton catalyst-based nanocarriers could be degraded and release Fenton catalysts in the acidic tumor microenvironment, thereby catalyzing intracellular H_2O_2 decomposition and generating abundant toxic $\bullet OH$ (Fig. 1). These typical metal catalysts have been widely studied, and they have shown excellent $\bullet OH$ generation for inducing cancer oxidative stress and apoptosis [23–26]. Although tumor cells are characterized by the over-expression of H_2O_2 , the amount of $\bullet OH$ needed to achieve the desired therapeutic outcomes still cannot be produced. Therefore, elevating H_2O_2 levels to produce considerable $\bullet OH$ is a feasible approach to improve therapeutic effectiveness. Many strategies have been designed to elevate H_2O_2 levels in tumor sites for cancer treatment [27–33].

Received February 3, 2021; accepted June 1, 2021

E-mails: wangzheng2006@tju.edu.cn (Wang Z),
Dunyunshi01@gmail.com (Shi D)

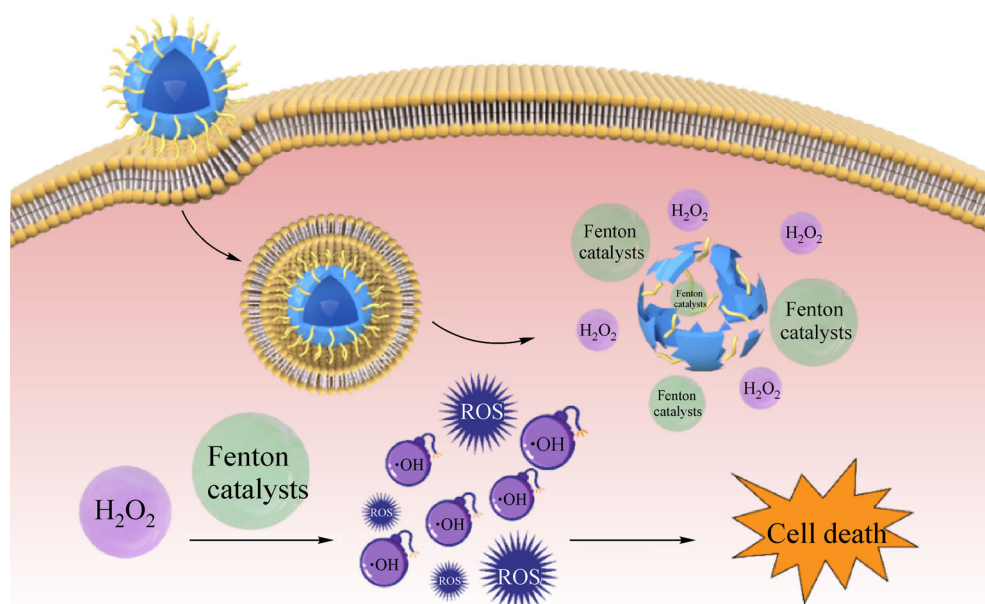


Fig. 1 Schematic illustration of $\bullet\text{OH}$ -mediated cancer therapy.

This review aims to highlight different strategies for boosting $\bullet\text{OH}$ generation. On one hand, we focus on the supply of typical metal-based Fenton catalysts to promote $\bullet\text{OH}$ generation. On the other hand, we emphasize on the synergistic elevation of H_2O_2 level to boost $\bullet\text{OH}$ generation, thereby achieving satisfactory therapeutic performance. Finally, the limitations and improvement of hydroxyl radical-based cancer therapy are also discussed.

2 Introduction of Fenton catalysts

Intracellular H_2O_2 can be converted into $\bullet\text{OH}$ by introducing Fenton catalysts. Therefore, supplying Fenton catalysts to the tumor sites is an effective strategy to promote $\bullet\text{OH}$ generation. Many research groups have investigated the efficacy of classical metal Fenton catalyst-based nanocarriers to enable $\bullet\text{OH}$ generation (shown in Table 1).

According to the sources of Fenton catalysts, three classical metal types are mainly summarized in Fig. 2: Fe-based Fenton catalysts, Mn-based Fenton catalysts, and Cu-based Fenton catalysts. We review the Fenton catalysts based on three types in the following.

2.1 Fe-based Fenton catalysts

Iron ions as the classical Fenton catalyst have been extensively applied in $\bullet\text{OH}$ generation. With the development of nanotechnology, various nanocarriers have been developed and applied in antitumor therapy [83–85]. Fe-based nanocarriers have been constructed and proven effective in generating $\bullet\text{OH}$ because of the presence of iron

ions, including iron oxide NPs [34,35,86], iron-based metal-organic frameworks [36], and other iron-based nanocarriers [37,38]. These iron-based nanocarriers have good magnetic targeting ability, specifically targeting cancer cells. Hence, iron-based nanocarriers could accumulate at the tumor sites to target the release of iron ions, thereby promoting $\bullet\text{OH}$ production. Moreover, the released iron ions show the function of nuclear magnetic imaging, monitoring the therapeutic process.

As an example for iron oxide NPs, Yu et al. constructed pH-sensitive $\text{Fe}_5\text{C}_2@\text{Fe}_3\text{O}_4$ NPs that could be adequately decomposed, promoting the release of Fe^{2+} in acidic tumor conditions. As shown in Fig. 3, the constructed $\text{Fe}_5\text{C}_2@\text{Fe}_3\text{O}_4$ nanocarriers had high sensitivity to the acidity of tumor sites, effectively releasing Fe^{2+} in tumor regions. The released Fe^{2+} could react with overexpressed H_2O_2 to produce $\bullet\text{OH}$, specifically killing cancer cells and showing an excellent antitumor effect. Considering that the release of iron ions from $\text{Fe}_5\text{C}_2@\text{Fe}_3\text{O}_4$ depended on low pH, the toxicity of $\text{Fe}_5\text{C}_2@\text{Fe}_3\text{O}_4$ was minimal in normal cells [39]. The designed nanocarriers provided a new strategy for efficient and specific cancer therapy based on the selective catalysis of $\bullet\text{OH}$ generation.

In addition to Fe-based nanocarriers, Fc and its derivatives can generate $\bullet\text{OH}$ and simultaneously release Fe^{2+} in the presence of H_2O_2 and H^+ . Therefore, numerous nanocarriers designed on the basis of Fc and its derivatives have been applied in anticancer treatments [40–45,87]. For example, Chen et al. constructed a new nanodrug ($\text{GOx}\&\text{Pt}@\text{FcNV}$) using a Fc-containing nanovesicle. As shown in Fig. 4, the $\text{GOx}\&\text{Pt}@\text{FcNV}$ nanodrug could deliver GOx, Fc and cisplatin (Pt) into the tumor sites. The GOx-mediated starvation therapy could consume intracel-

Table 1 The supply of Fenton catalysts and elevation of H₂O₂ level for enhanced •OH generation ^{a)}

Material	Functional mechanism	Cell	Ref.
IONPs	Fe ²⁺ -mediated •OH generation	HT1080	[34]
JFSNs-GOx	GOx-catalyzed H ₂ O ₂ generation; Fe ²⁺ -mediated •OH generation	4T1	[35]
CPT@MOF(Fe)-GOx	GOx-catalyzed H ₂ O ₂ generation; Fe ²⁺ -mediated •OH generation; CPT-mediated chemotherapy	HeLa	[36]
rFeO _x -HMSN	Fe ²⁺ -mediated •OH generation	4T1	[37]
LET-6	Fe ²⁺ -mediated •OH generation; tPy-Cy-Fe-mediated photothermal therapy	U87MG	[38]
Fe ₃ C ₂ @Fe ₃ O ₄ NPs	Fe ²⁺ -mediated •OH generation	4T1	[39]
FDMSNs@GOx@HA	GOx-catalyzed H ₂ O ₂ generation; Fe ²⁺ -mediated •OH generation	L-02; HeLa	[40]
Fe-CO@Mito-PNBE	CO-mediated gas therapy; Fe ²⁺ -mediated •OH generation	4T1; HeLa	[41]
CuS-Fe@polymer	Fe ²⁺ -mediated •OH generation; CuS-mediated photothermal therapy	HeLa; NIH3T3	[42]
Co-Fc@GOx	GOx-catalyzed H ₂ O ₂ generation; Fe ²⁺ -mediated •OH generation	HUVEC; 4T1	[43]
Zr-Fc MOF	Zr-Fc MOF-mediated photothermal therapy; Fe ²⁺ -mediated •OH generation	7702; 4T1; Huh7	[44]
CFNCs	Fe ²⁺ -mediated •OH generation; PTX-mediated chemotherapy	HCT-15; NIH3T3	[45]
GOx&Pt@FcNV	GOx-catalyzed H ₂ O ₂ generation; Fe ²⁺ -mediated •OH generation; Pt-mediated chemotherapy	A549; MCF7	[46]
GOx@ZIF@MPN	GOx-catalyzed H ₂ O ₂ generation; Fe ²⁺ -mediated •OH generation	4T1	[47]
BSO/GA-Fe(II)@liposome	BSO-mediated GSH synthesis inhibition; Fe ²⁺ -mediated •OH generation	4T1	[48]
SRF@Fe ^{III} TA	SRF-mediated GSH synthesis inhibition; Fe ²⁺ -mediated •OH generation	4T1; CT26; HepG2; 3T3; COS7; NCTC 1469	[49]
Fe ³⁺ -DOX@EGCG-PEG NPs	DOX-mediated chemotherapy; Fe ²⁺ -mediated •OH generation	U87MG; 293T	[50]
DOX/Fe ³⁺ /EGCG NPs	DOX-mediated chemotherapy; Fe ²⁺ -mediated •OH generation	LL2; A549	[51]
MnS@BSA	H ₂ S-mediated gas therapy; Mn ²⁺ -mediated •OH generation	4T1	[52]
GOx-MnCaP-DOX	GOx-catalyzed H ₂ O ₂ generation; Mn ²⁺ -mediated •OH generation; DOX-mediated chemotherapy	4T1	[53]
GNR@SiO ₂ @MnO ₂	Mn ²⁺ -mediated •OH generation; GSM-mediated photothermal therapy	U87MG	[54]
BMC-DOX	Mn ²⁺ -mediated •OH generation; DOX-mediated chemotherapy	4T1; U87MG	[55]
GMCD	GOx-catalyzed H ₂ O ₂ generation; Mn ²⁺ -mediated •OH generation; CAT-mediated O ₂ generation; DVDMS-mediated ¹ O ₂ generation	4T1	[56]
MS@MnO ₂ NPs	MnO ₂ -mediated GSH depletion; Mn ²⁺ -mediated •OH generation	U87MG	[57]
PCN-224(Cu)-GOD@MnO ₂	MnO ₂ -mediated O ₂ supply; GOD-mediated H ₂ O ₂ generation; Cu ⁺ -mediated •OH generation	L929; HeLa	[58]
Cu _{2-x} S-PEG NDs	Cu _{2-x} S-mediated photothermal therapy; Cu ⁺ -mediated •OH generation	4T1	[59]
PEG-Cu ₂ Se HNCs	Cu ₂ Se-mediated photothermal therapy; Cu ⁺ -mediated •OH generation	HUVECs; 4T1	[60]
PGC-DOX	GOx-catalyzed H ₂ O ₂ generation; Cu ²⁺ -mediated GSH depletion; Cu ⁺ -mediated •OH generation; DOX-mediated chemotherapy	4T1	[61]
SC@G NSs	GOx-catalyzed H ₂ O ₂ generation; Sr ⁺ /Cu ⁺ -mediated •OH generation; SC NSs-mediated photothermal therapy	4T1; 293T	[62]
Cu-Cys NPs	Cu ²⁺ -mediated GSH depletion; Cu ⁺ -mediated •OH generation	HeLa; MCF-7; PC-3; hADSCs; hbMSCs; HK-2	[63]
GOD-Fe ₃ O ₄ @DMSNs	GOD-catalyzed H ₂ O ₂ generation; Fe ²⁺ -mediated •OH generation	4T1; U87	[64]

(Continued)

Material	Functional mechanism	Cell	Ref.
MNS-GOx	GOx-catalyzed H ₂ O ₂ generation; Mn ²⁺ -mediated •OH generation	A375	[65]
Fe ₅ C ₂ -GOD@MnO ₂	MnO ₂ -mediated O ₂ supply; GOD-mediated H ₂ O ₂ generation; Fe ²⁺ -mediated •OH generation	HeLa	[66]
PEG-Au/FeMOF@CPT NPs	Au-catalyzed H ₂ O ₂ generation; Fe ²⁺ -mediated •OH generation; CPT-mediated chemotherapy	HepG2	[67]
DMSN-Au-Fe ₃ O ₄ -PEG NPs	Au-catalyzed H ₂ O ₂ generation; Fe ²⁺ -mediated •OH generation	4T1	[68]
Fe ₃ O ₄ @PEI-Pt(IV)-PEG	SOD-catalyzed H ₂ O ₂ generation; Fe ²⁺ -mediated •OH generation; Pt-mediated chemotherapy	A2780; ACP	[69]
PZIF67-AT	As nanozyme, ZIF-67-mediated H ₂ O ₂ generation, •OH generation, and GSH depletion; 3-AT-mediated H ₂ O ₂ elimination inhibition	A549; HeLa; 4T1	[70]
PA/Fc-Micelles	Asc-mediated H ₂ O ₂ generation; Fe ²⁺ -mediated •OH generation	4T1; MCF-7	[71]
CaP-Fe/RSL3 + Asc	Asc-mediated H ₂ O ₂ generation; Fe ²⁺ -mediated •OH generation; RSL3-mediated GPX4 inhibition	4T1	[72]
CaO ₂ -Fe ₃ O ₄ @HA NPs	CaO ₂ -mediated H ₂ O ₂ generation; Fe ²⁺ -mediated •OH generation	4T1; NIH/3T3; LO2; MCF-7	[73]
Nb ₂ C-IO-CaO ₂ -PVP	CaO ₂ -mediated H ₂ O ₂ generation; Fe ²⁺ -mediated •OH generation	4T1	[74]
CP nanodots	CP nanodots -mediated H ₂ O ₂ generation and •OH generation	U87MG	[75]
Fe-GA/CaO ₂ @PCM	PCMs-mediated photothermal-responsive gatekeeper; CaO ₂ -mediated H ₂ O ₂ generation; Fe ²⁺ -mediated •OH generation	HeLa	[76]
HA-CD/Fc-CA NPs	CA-mediated H ₂ O ₂ generation; Fe ²⁺ -mediated •OH generation	MCF-7; 4T1; NIH/3T3	[77]
PolyCAFe	CA-mediated H ₂ O ₂ generation; Fe ²⁺ -mediated •OH generation	SW620; DU145; HEK293; NIH3T3	[78]
LaCIONPs	La-mediated H ₂ O ₂ generation; Fe ²⁺ -mediated •OH generation; CPT-mediated chemotherapy	A549	[79]
PtkDOX-NMs	La-mediated H ₂ O ₂ generation; Fe ²⁺ -mediated •OH generation; DOX-mediated chemotherapy	A549	[80]
Fe ₃ O ₄ -HSA@Lapa	La-mediated H ₂ O ₂ generation; Fe ²⁺ -mediated •OH generation	A549	[81]
Fe@Fe ₃ O ₄ @Cu _{2-x} S@La-PEG	La-mediated H ₂ O ₂ generation; Fe@Fe ₃ O ₄ @Cu _{2-x} S-PEG-mediated •OH generation	4T1; HUVE	[82]

a) GOD or GOx: glucose oxidase; La: β -lapachone; CA: cinnamaldehyde; CAT: catalase; GPX: glutathione peroxidase; NP: nanoparticle; Fc: ferrocene; DOX: doxorubicin; GSH: glutathione; Asc: ascorbate; GA: gallic acid; PCMs: phase change materials; MOF: metal-organic framework; EGCG: epigallocatechin gallate; ZIF: zeolite imidazole framework; 3-AT: 3-amino-1,2,4-triazole.

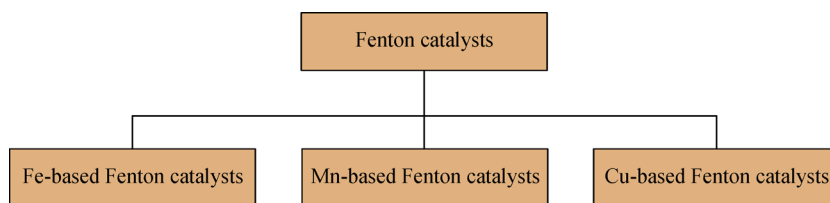


Fig. 2 Three typical metal-based catalysts for the Fenton reaction.

lular glucose to concurrently generate H₂O₂ and H⁺, accelerating the release of Fe²⁺ from Fc. The released Fe²⁺ could catalyze H₂O₂ decomposition into •OH, resulting in the apoptosis of cancer cells. Moreover, the Pt-mediated chemotherapy would enhance the therapeutic effect [46]. This designed therapeutic strategy offered a new angle for the endogenous stimuli-activated nanocarriers to combat multidrug-resistant tumors.

In iron-mediated •OH generation, Fe²⁺ exists much better catalytic activity than Fe³⁺. However, Fe²⁺ is unstable and easily oxidized [88]. Consequently, elevating Fe²⁺ content is a feasible approach to promote •OH generation. Given the effectivity of iron redox cycling, a simultaneous supply of iron ions and some reductants has been received widespread attention, such as tannic acid, EGCG and GA [47–49]. These reductants are mostly

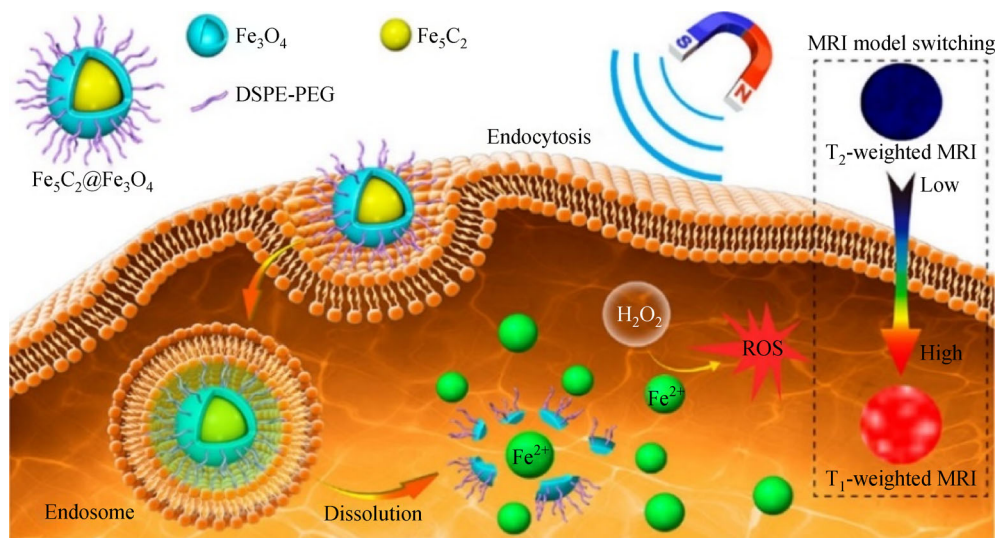


Fig. 3 Schematic diagram of the therapeutic mechanism of $\text{Fe}_5\text{C}_2@\text{Fe}_3\text{O}_4$ NPs. Reprinted with permission from ref. [39]. Copyright 2019, American Chemical Society.

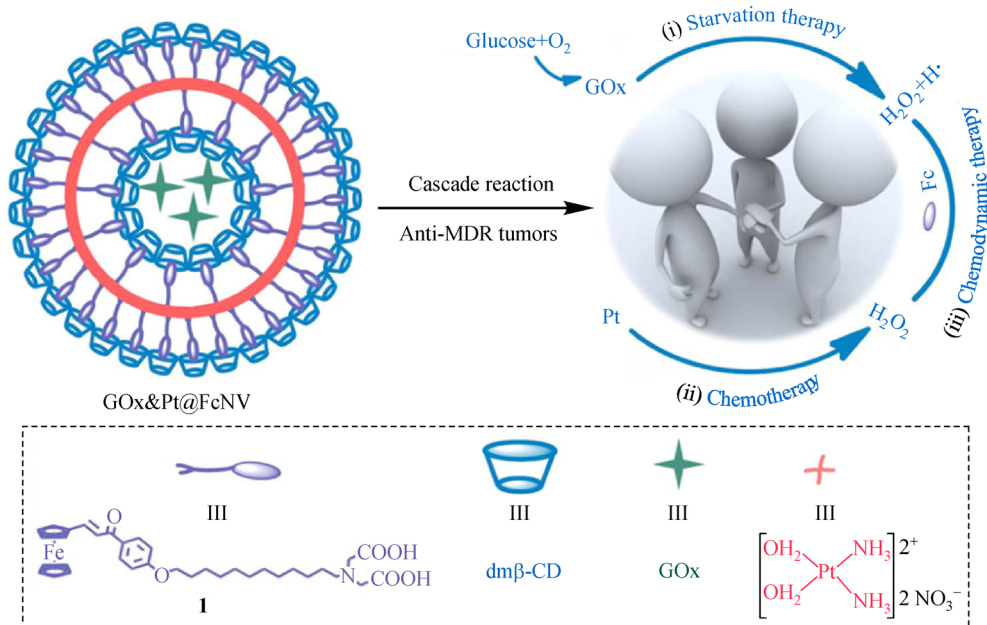


Fig. 4 Schematic illustration of the mechanisms of $\text{GOx}\&\text{Pt}\&\text{FcNV}$ against tumors. Reprinted with permission from ref. [46]. Copyright 2019, American Chemical Society.

polyphenolic compounds, which can chelate Fe^{3+} to form metal polyphenol network nanocarriers [50]. The formed nanocarriers show excellent aqueous dispersion due to the presence of phenolic hydroxyl groups. The chelation forces between polyphenol and Fe^{3+} can easily break in acidic conditions, resulting in the release of polyphenol and Fe^{3+} . The released Fe^{3+} can be reduced into Fe^{2+} by polyphenol compounds, achieving Fe^{2+} -supply-regeneration cycling [89].

As an interesting paradigm, Mu et al. designed and synthesized $\text{DOX}/\text{Fe}^{3+}/\text{EGCG}$ NPs using a one-pot green

method. DOX , EGCG and Fe^{3+} could be simultaneously delivered into the tumor sites via the formed nanocarriers. After endocytosis into tumor cells, the $\text{DOX}/\text{Fe}^{3+}/\text{EGCG}$ NPs could be degraded and release DOX , EGCG and Fe^{3+} under high GSH and acidic conditions (Fig. 5). The liberated EGCG -mediated Fe^{2+} generation could effectively achieve Fe^{2+} -cycling supply. The Fe^{2+} -mediated $\cdot\text{OH}$ generation via the Fenton reaction could rapidly promote cancer cell death. Moreover, DOX -mediated chemotherapy could enhance the effect of tumor treatment. The experimental results demonstrated that $\text{DOX}/\text{Fe}^{3+}/$

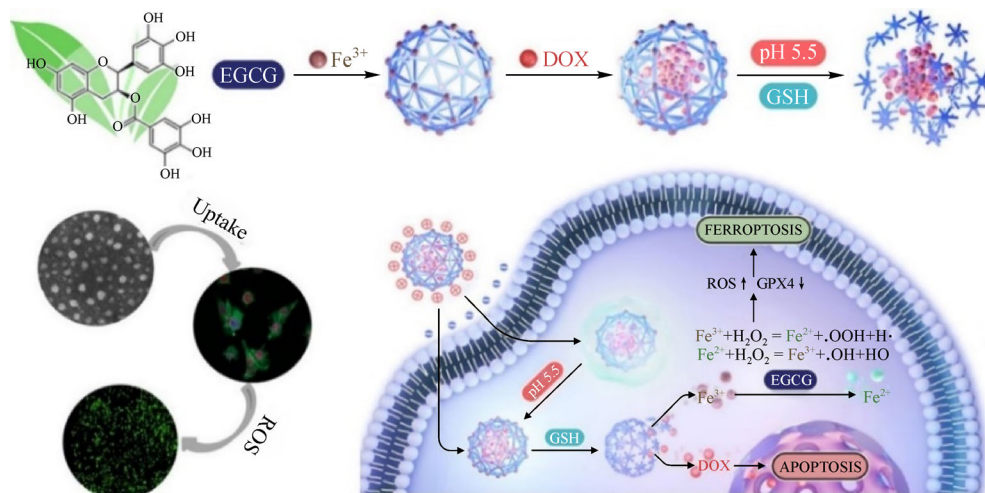


Fig. 5 Schematic illustration of the synthetic process and the therapeutic mechanism of the DOX/Fe³⁺/EGCG NPs. Reprinted with permission from ref. [51]. Copyright 2020, American Chemical Society.

EGCG NPs had a remarkable antitumor effect [51]. The therapeutic strategy provided new insights into the effective Fe²⁺ supply to tumor sites.

2.2 Mn-based Fenton catalysts

The tumor microenvironment features low pH, over-produced H₂O₂ and a high GSH concentration. The generated •OH can be eliminated by intracellular GSH, significantly reducing the curative effects [90]. Consequently, developing a novel treatment method to enhance •OH accumulation by promoting GSH consumption and increasing •OH generation is necessary. According to literature reports, Mn-based nanomaterials could react with intracellular GSH, promoting GSH depletion and Mn²⁺ generation. The produced Mn²⁺ could catalyze H₂O₂ decomposition into •OH in the presence of HCO₃⁻ via the Fenton-like reaction. Therefore, Mn-based nanomaterials could induce GSH depletion and enhance •OH accumulation. Given their excellent advantages, Mn-based nanocarriers could be used as Fenton catalysts [52–56,91].

As an example, Lin et al. obtained the MS@MnO₂ NPs by wrapping mesoporous silica on the surface of MnO₂. As depicted in Fig. 6, MnO₂ was easily disintegrated by intracellular GSH, inducing GSH depletion and Mn²⁺ release. The GSH depletion enhanced the accumulation of Mn²⁺-mediated •OH generation. The results *in vitro* and *in vivo* indicated that MS@MnO₂ NPs exhibited significant anticancer efficacy. This work provided a paradigm to design Fenton catalyst-based nanoagents with the ability to deplete intracellular GSH for enhanced •OH accumulation [57]. Mn-based nanocarriers as Fenton catalysts existed excellent antitumor effectiveness, which could attribute to their excellent Mn²⁺ delivery and GSH depletion capabilities, resulting in the •OH accumulation.

2.3 Cu-based Fenton catalysts

The •OH generation is not only restricted by limited catalytic ions and high content of GSH in tumor cells but also restrained by undesirable pH conditions of the Fenton reaction [92,93]. The occurrence of Fenton reaction requires a low pH (3–4). Hence, a slightly acidic tumor microenvironment can limit •OH generation, reducing antitumor effectiveness. Consequently, developing a new Fenton catalyst to generate abundant •OH in a weakly acidic condition is highly desired. Based on the published literature, Cu⁺ with reductive ability could react with intracellular H₂O₂ to generate •OH in a broad pH range [94]. However, Cu⁺ was unstable and prone to be oxidized into Cu²⁺. Thereby, Cu-based nanocarriers were generally introduced into cells in the form of Cu²⁺. The introduced Cu²⁺ could be transformed into Cu⁺ in the presence of GSH, which could promote GSH depletion to destroy the intracellular oxidative balance, promoting the accumulation of the generated •OH [95]. Cu-based nanomaterials were constructed to boost •OH generation such as copper-based metal-organic frameworks [58,96], copper sulfides, copper selenium [59,60], and other copper-based nanocarriers [61,62].

As an example, Ma and co-workers designed and synthesized Cu-Cys NPs through the self-assembled copper-amino acid mercaptide for GSH-activated and H₂O₂-reinforced •OH generation. As shown in Fig. 7, Cu-Cys NPs could react with excess intracellular GSH to induce the depletion of GSH and generation of Cu⁺. Subsequently, the generated Cu⁺ could react with endogenous H₂O₂ to produce highly oxidative •OH with a rapid reaction rate in the faintly acidic microenvironment, efficiently inducing apoptosis of cancer cells. The *in vitro* and *in vivo* results indicated that Cu-Cys NPs exhibited

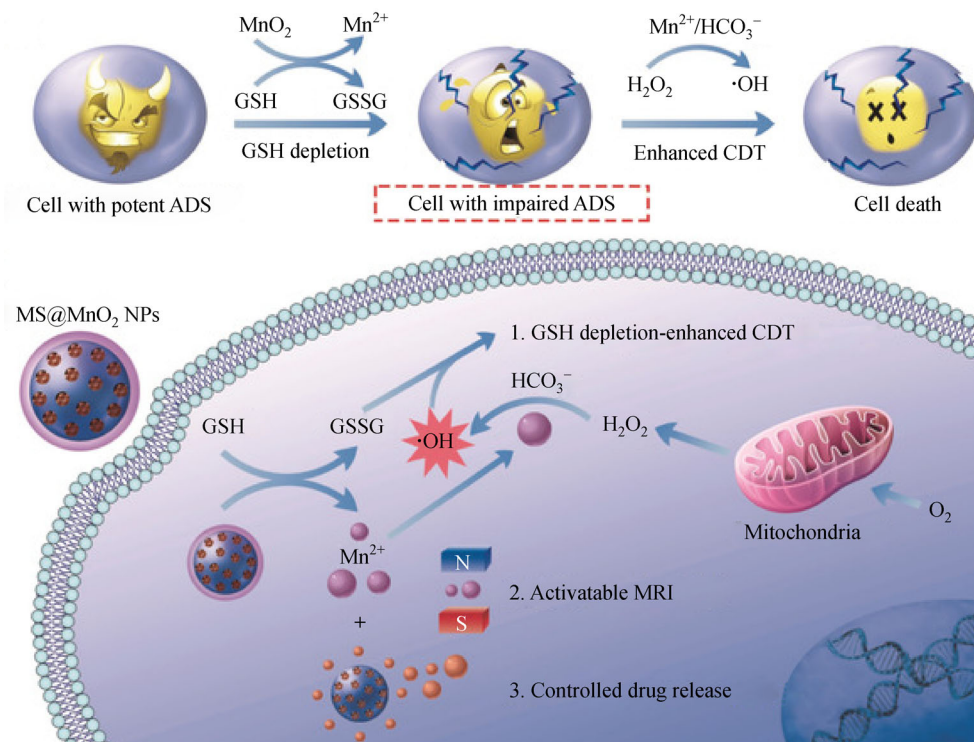


Fig. 6 Schematic illustration of the mechanism of MS@MnO₂ NPs for combination therapy. Reprinted with permission from ref. [57]. Copyright 2018, John Wiley and Sons.

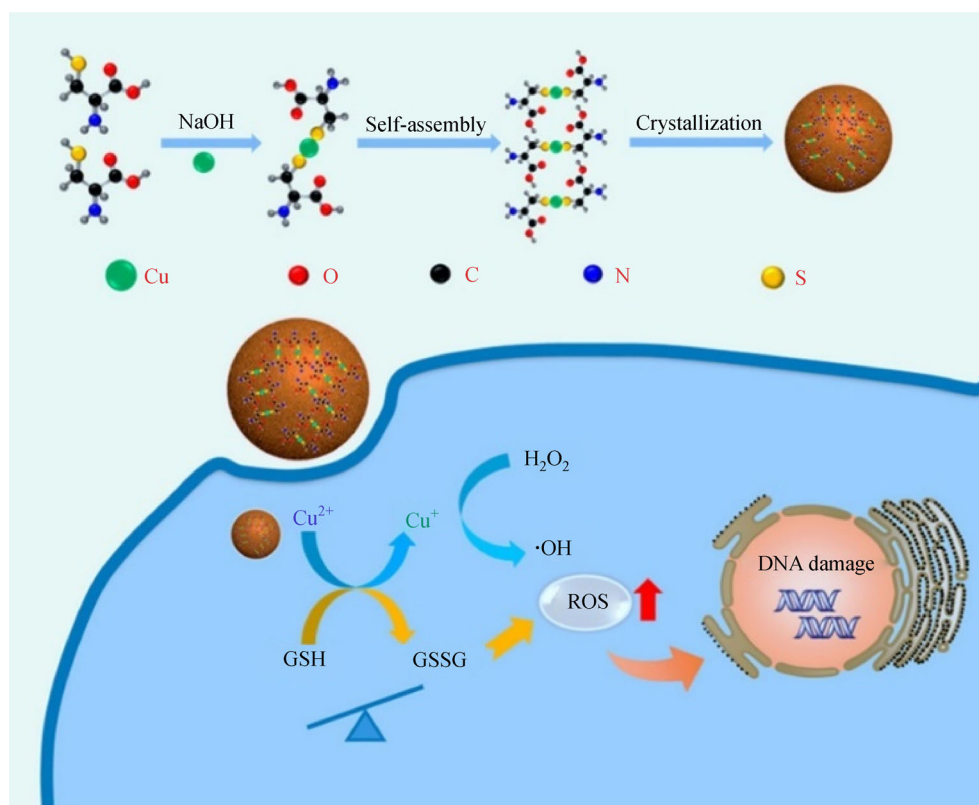


Fig. 7 Schematic illustration of the synthetic process and the therapeutic mechanism of the Cu-Cys NPs. Reprinted with permission from ref. [63]. Copyright 2019, American Chemical Society.

relatively high cytotoxicity to cancer cells, showing efficient tumor growth suppression [63]. The designed nanocarrier that responsive to tumor microenvironment showed potential application in $\bullet\text{OH}$ -mediated antitumor therapy. Cu^+ -mediated Fenton reaction could occur in the wide pH range to generate $\bullet\text{OH}$, improving the efficiency of $\bullet\text{OH}$ generation and the therapeutic effect.

3 Elevation of H_2O_2 level for enhanced $\bullet\text{OH}$ generation

The effective $\bullet\text{OH}$ generation relies not only on the supply of Fenton catalysts but also on sufficient H_2O_2 as reaction substrates. Although H_2O_2 is overexpressed in tumor sites, it is still insufficient to generate considerable $\bullet\text{OH}$ to achieve satisfying therapeutic performance. Therefore, facilitating H_2O_2 production in the tumor region can address insufficient endogenous H_2O_2 and promote abundant $\bullet\text{OH}$ generation. Plentiful therapeutic strategies have been designed to increase intracellular H_2O_2 levels (Table 1). For instance, GOD can effectively catalyze intracellular glucose oxidation to produce gluconic acid and H_2O_2 [97]. Moreover, as an artificial enzyme, ultrasmall Au NPs can have specific GOD-like catalytic activity, which can also catalyze glucose oxidation to boost H_2O_2 generation [98,99]. Superoxide dismutase (SOD) or SOD-like enzyme can convert intracellular $\text{O}_2^{\cdot-}$ into H_2O_2 , increasing H_2O_2 amounts [100–102].

Except for the above-mentioned enzymes, Asc [103] and metal peroxides (MO_2) [104,105] have been aroused attention in the ability of H_2O_2 elevation due to their higher stability and lower cost. Organic compounds, including CA and La, can elevate intracellular H_2O_2 content. Based on the mechanism of H_2O_2 generation, strategies for the upregulation of H_2O_2 levels are summarized in Fig. 8.

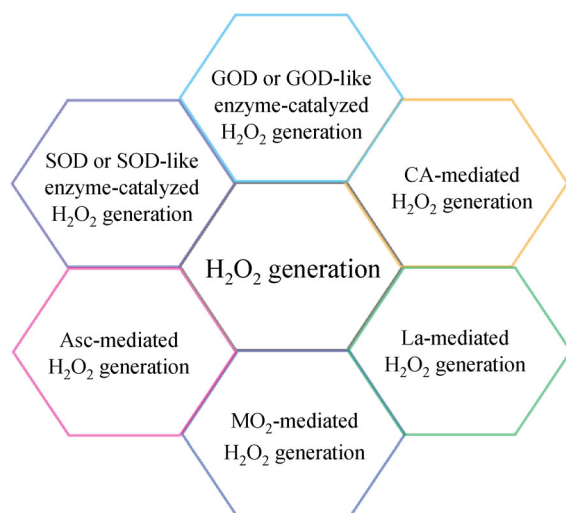


Fig. 8 Schematic illustration of various strategies to boost H_2O_2 generation.

3.1 Glucose oxidase or glucose oxidase-like enzyme-catalyzed H_2O_2 generation

As an endogenous oxidoreductase, GOD comprises two identical polypeptide chain subunits and flavin adenine dinucleotide coenzymes, specifically catalyzing intracellular β -D-glucose oxidation to produce gluconic acid and H_2O_2 in the presence of O_2 and H_2O [64,106–109]. The therapeutic strategies based on GOD-mediated H_2O_2 generation have been used in cancer therapy [65,110–113]. According to the catalytic mechanism, the GOD-catalyzed H_2O_2 generation requires the participation of O_2 . However, given the hypoxic characteristic of the tumor microenvironment, the efficacy of GOD-catalyzed H_2O_2 generation is significantly hindered. Consequently, increasing intracellular O_2 content is a suitable approach to improve the efficiency of GOD-catalyzed H_2O_2 production.

As an example, Lin's group synthesized multifunctional nanocarriers using Fe_5C_2 -GOD as the core and pH-responsive MnO_2 as the outer shell to form Fe_5C_2 -GOD@ MnO_2 (Fig. 9). Upon entering tumor cells, the acidic microenvironment could decompose the MnO_2 to generate O_2 , simultaneously inducing the GOD release and the Fe^{2+} release from Fe_5C_2 NPs. The generated O_2 would promote GOD-catalyzed glucose oxidation to enhance H_2O_2 generation and decrease intracellular pH. Decreasing pH and generating H_2O_2 would speed up Fe^{2+} -catalyzed $\bullet\text{OH}$ generation, further triggering cancer cell death. The experimental results suggested that Fe_5C_2 -GOD@ MnO_2 exhibited an excellent antitumor effect due to the MnO_2 -mediated O_2 supply and GOD-activated H_2O_2 production for reinforced Fe^{2+} -mediated $\bullet\text{OH}$ generation [66]. The designed Fe_5C_2 -GOD@ MnO_2 nanocarriers provided a potential strategy to improve tumor-specific $\bullet\text{OH}$ production and minimize side effects on normal tissues.

However, as a natural enzyme, GOD can be easily inactivated under severe conditions, restricting its application. The ultrasmall Au NPs as an artificial nanozyme have attracted attention by virtue of their specific GOD-like catalytic activity, high stability, and significant catalytic activity against harsh conditions [67,114–117]. As an example, Gao et al. designed and synthesized the cascade catalytic nanoplatform by integrating 1.5 nm Au NPs and ultrasmall Fe_3O_4 NPs into DMSN NPs with large pore channels to construct DMSN-Au- Fe_3O_4 NPs. The PEG was further modified on the surface of DMSN-Au- Fe_3O_4 NPs to improve the stability (Fig. 10). The formed DMSN-Au- Fe_3O_4 -PEG NPs could trigger intracellular cascade catalytic reaction under the tumor microenvironment. Au NPs as a GOD-like nanozyme could catalyze intracellular glucose oxidation to generate gluconic acid and H_2O_2 . The decrease in pH would promote $\bullet\text{OH}$ generation via the Fenton reaction between ultrasmall Fe_3O_4 NPs and H_2O_2 , triggering tumor cell death. Extensive evaluations *in vitro* and *in vivo* demonstrated that the DMSN-Au- Fe_3O_4 -PEG

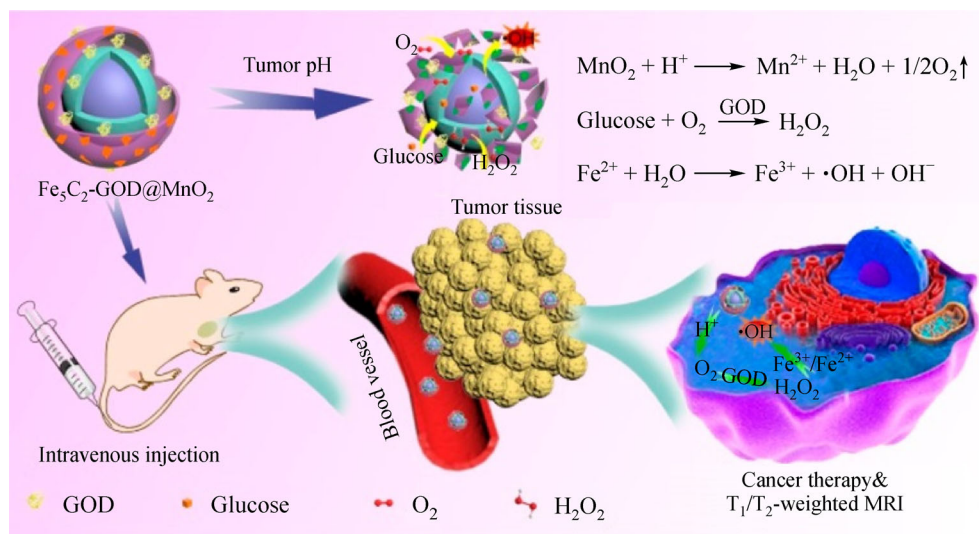


Fig. 9 Schematic diagram of the therapeutic mechanism of $\text{Fe}_5\text{C}_2\text{-GOD@MnO}_2$ nanocarriers. Reprinted with permission from ref. [66]. Copyright 2018, American Chemical Society.

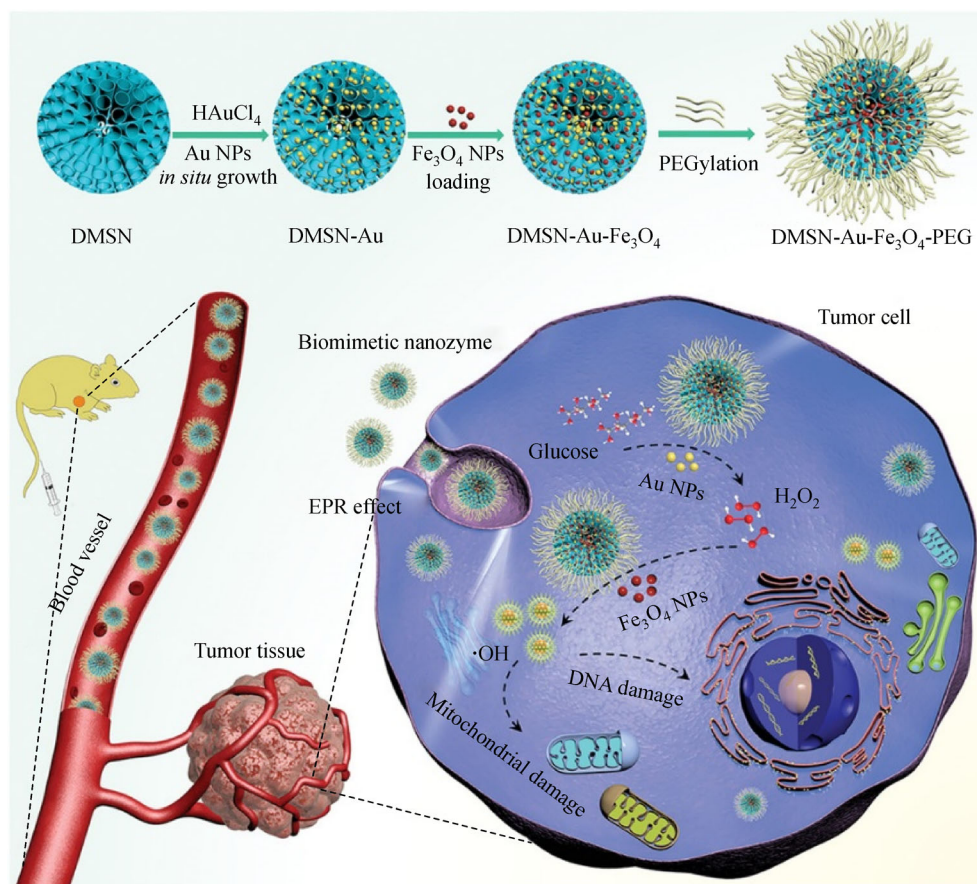


Fig. 10 Schematic illustration of the synthetic process and the therapeutic mechanism of the DMSN-Au- Fe_3O_4 -PEG NPs. Reprinted with permission from ref. [68]. Copyright 2019, John Wiley and Sons.

NPs showed excellent therapeutic effects with a tumor suppression rate of 69.08% and without additional side effects [68]. Therefore, tumor microenvironment-triggered nanocarrier not only provided a “toxic-drug-free” therapeutic strategy but also stimulated the development of tumor-specific therapies.

3.2 SOD or SOD-like enzyme-catalyzed H_2O_2 generation

Intracellular O_2^- can react with H^+ to form H_2O_2 during the catalysis of SOD [118]. Hence, SOD or SOD-like enzyme can increase the intracellular H_2O_2 concentration [119,120]. Inspired by this principle of H_2O_2 formation, Ma et al. constructed the $\text{Fe}_3\text{O}_4@\text{PEI-Pt(IV)-PEG}$ (FePt-NP2) nanocarrier with a hydrodynamic size of 252 nm. As depicted in Fig. 11, once injected into cancer tissues, FePt-NP2 could be decomposed in an acidic microenvironment, liberating iron ions and Pt. The liberated Pt-mediated O_2^- generation and chemotherapy could enhance antitumor efficacy. The formed O_2^- could be converted into H_2O_2 under the catalysis of SOD. The up-regulation of H_2O_2 content could accelerate the $\bullet\text{OH}$ generation between the released iron ions and H_2O_2 , inducing tumor cell death. The synthesized sequential drug delivery nanocarriers could achieve tumor site-specific ROS generation utilizing the supply of iron ions and the elevation of H_2O_2 content, enhancing anticancer effect. The *in vitro* and *in vivo* results demonstrated that FePt-NP2 showed outstanding antitumor outcomes and potential application in cancer therapy [69]. This work provided a promising delivery method for synergistic therapy. Besides SOD enzyme, the SOD-like enzyme could catalyze O_2^- to form H_2O_2 , elevating intracellular H_2O_2 content. For example, Sang et al. synthesized ZIF-67 NPs with SOD-like activity and Fenton-like catalytic activity. As shown in Fig. 12, the synthesized ZIF-67 could catalyze intracellular O_2^- to

generate H_2O_2 . Moreover, the elevated H_2O_2 could be sequentially converted into $\bullet\text{OH}$ in the presence of ZIF-67. To improve the therapeutic effect and increase the stability, 3-AT and PEG were modified on the surface of ZIF-67 (named PZIF67-AT). On one hand, 3-AT as the CAT inhibitor could suppress H_2O_2 decomposition. On the other hand, PZIF67-AT-mediated GSH depletion could also prohibit H_2O_2 clearance [70]. The inhibition of H_2O_2 clearance had been proven to significantly increase $\bullet\text{OH}$ generation, achieving better therapeutical effects. This work provided new insights into the design of H_2O_2 -supplementing strategies.

3.3 Ascorbate-mediated H_2O_2 generation

Ascorbate (Asc) has been frequently utilized to elevate intracellular H_2O_2 levels. According to existing research reports, in extracellular fluid, Asc at the pharmacologic concentration could lose one electron and form Asc^- ; cellular O_2 could obtain an electron from M^n to form O_2^- ; M^n could simultaneously be reduced to M^{n-1} during this process; the intracellular H^+ subsequently could react with O_2^- to produce H_2O_2 and O_2 [71,121–126]. Asc-mediated H_2O_2 generation has received great attention due to its biosafety. Based on this mechanism, An and co-workers synthesized the hybrid nanocarriers by physically encapsulating polar ferric ammonium citrate and nonpolar RSL3 into the lipid-coated calcium phosphate (CaP) core and shell, respectively. The formed nanocarrier with a suitable particle size was named CaP-Fe/RSL3. As shown in Fig. 13, the hybrid nanocarriers could be quickly degraded in an acidic environment. Asc-induced selective enrichment of H_2O_2 coupled with Fe^{3+} co-delivery could boost the $\bullet\text{OH}$ levels in tumor sites. Simultaneous liberation of RSL3 as a GPX4 inhibitor could result in the accumulation of lipid peroxides, enhancing treatment efficacy. The *in vitro*

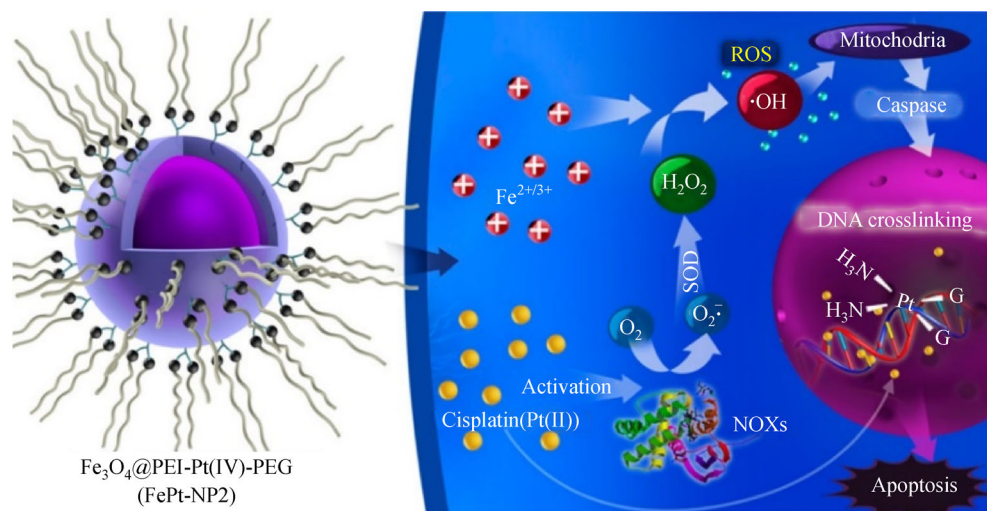


Fig. 11 Schematic diagram of the therapeutic mechanism of FePt-NP2 for synergistic actions. Reprinted with permission from ref. [69]. Copyright 2017, American Chemical Society.

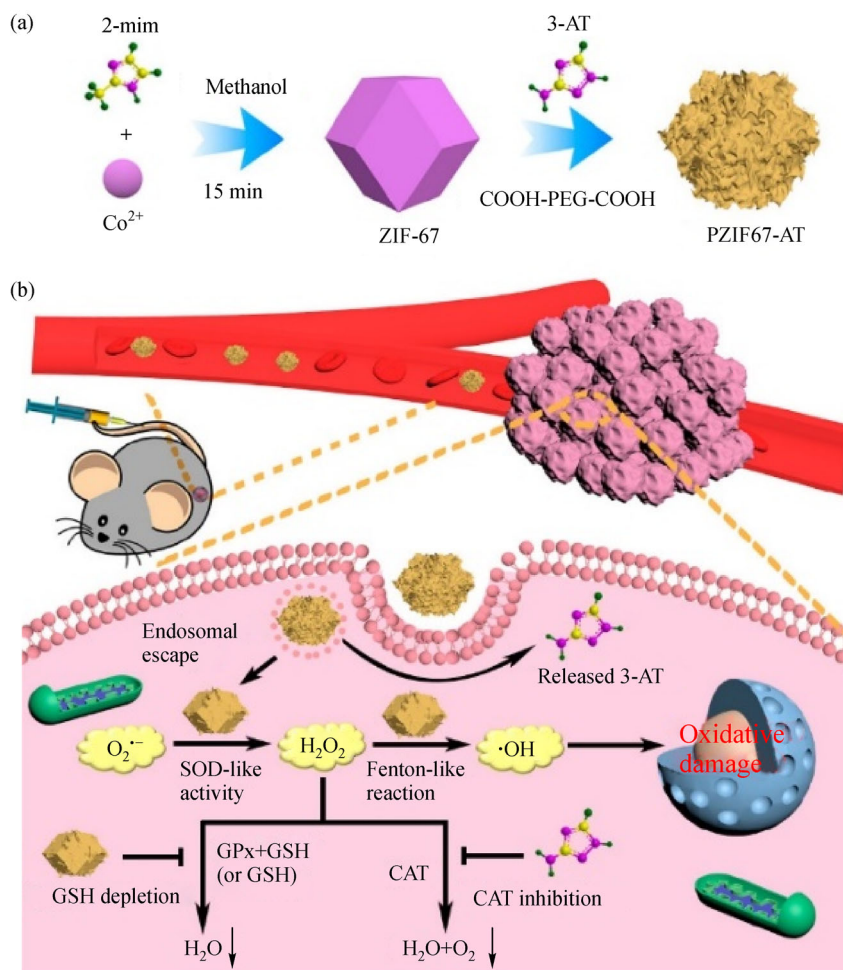


Fig. 12 Schematic representation of (a) the synthesis of PZIF67-AT NPs and (b) PZIF67-AT NPs-mediated intensive $\bullet\text{OH}$ production. Reprinted with permission from ref. [70]. Copyright 2020, American Chemical Society.

and *in vivo* results showed that Fe^{3+} delivery coupled with intraperitoneal administration of Asc had an excellent antitumor performance [72]. The combinational approach produced significantly elevated $\bullet\text{OH}$ levels, offering a new therapeutic method for enhancing therapeutic performance.

3.4 Metal peroxide-mediated H_2O_2 generation

The above-mentioned GOD or GOD-like enzyme, SOD or SOD-like enzyme, and Asc can promote H_2O_2 production, but these catalytic reactions severely depend on the cellular O_2 concentration [73,127–129]. However, hypoxia is regarded as a major feature of cancer cells, affecting the efficiency of H_2O_2 generation and reducing the therapeutic effect. Therefore, developing new therapeutic methods to overcome the hypoxic environment and increase H_2O_2 content is of importance. MO_2 are composed of $\text{O}_2^{\cdot-}$ and metal ions, which have been widely used to increase intracellular H_2O_2 content without the assistance of O_2 . The MO_2 can be dissociated to release metal ions and $\text{O}_2^{\cdot-}$

in acidic conditions. The released $\text{O}_2^{\cdot-}$ can react with H^+ to produce H_2O_2 . The MO_2 -based nanocarriers have been extensively used as H_2O_2 generators because of their simple preparation, low cost, and high stability [74,75,130]. Based on this, Zhang et al. fabricated Fe-GA/ CaO_2 @PCM nanocarriers with thermal responsiveness and self-sufficient H_2O_2 by utilizing organic PCMs to encapsulate Fe-GA NPs and ultra-small CaO_2 (Fig. 14). The thermally responsive PCMs melted with the increase of temperature, inducing the release of internal Fe-GA and CaO_2 . The liberated CaO_2 -mediated self-produced H_2O_2 would be transformed into $\bullet\text{OH}$ by reacting with Fe-GA to increase $\bullet\text{OH}$ levels, improving the antitumor effect. In addition, the Ca^{2+} -mediated mitochondrial damage could enhance the apoptosis of cancer cells. Due to the thermal-responsive feature, the designed Fe-GA/ CaO_2 @PCM could specifically release the inner drugs in tumor sites, avoiding the serious damage on normal cells [76]. Thus, MO_2 -based nanocarriers provided a new therapeutic strategy, specifically boosting H_2O_2 generation to improve the efficiency of $\bullet\text{OH}$ generation at hypoxic conditions.

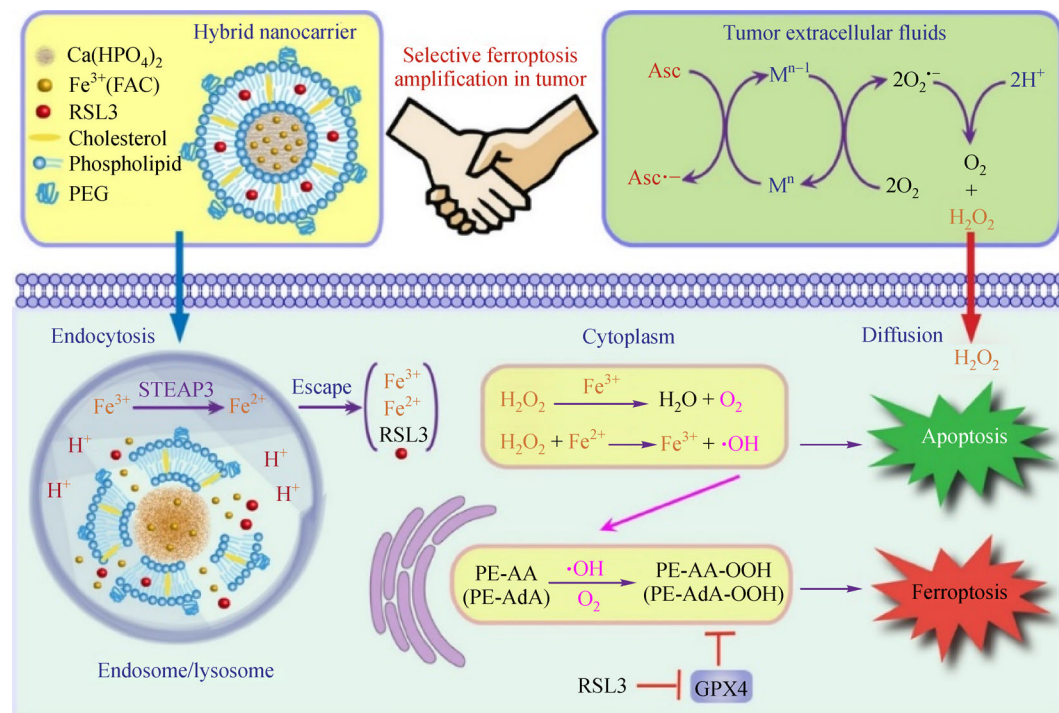


Fig. 13 Schematic illustration of the therapeutic mechanism of CaP-Fe/RSL3 + Asc. Reprinted with permission from ref. [72]. Copyright 2019, American Chemical Society.

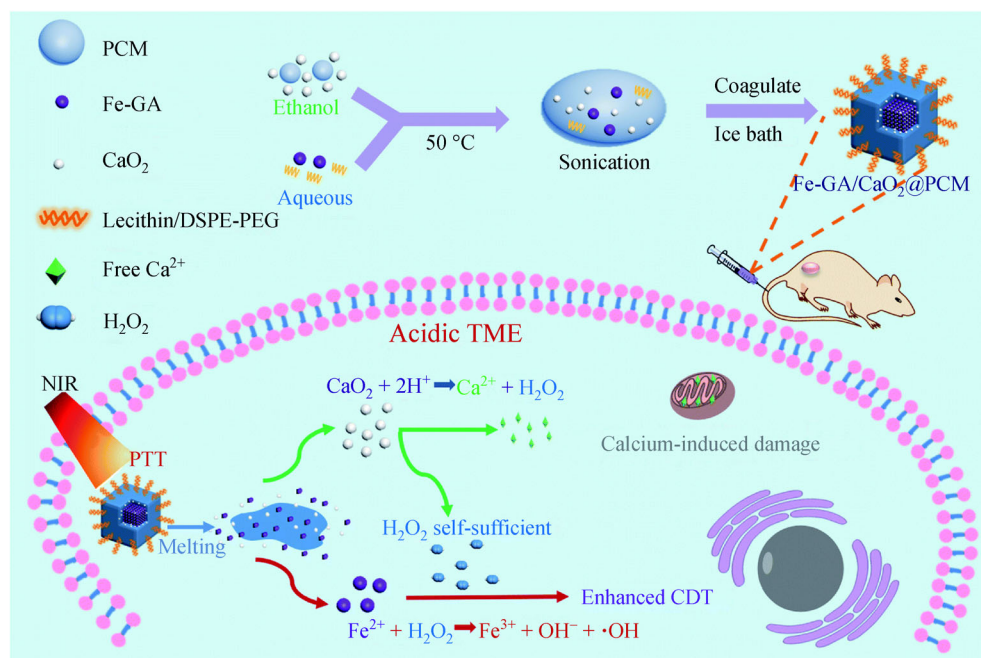


Fig. 14 Schematic illustration of the synthetic process and the therapeutic mechanism of Fe-GA/CaO₂@PCM. Reprinted with permission from ref. [76]. Copyright 2020, The Royal Society of Chemistry.

3.5 CA-mediated H₂O₂ generation

CA as a primary active ingredient of cinnamon, has been widely used as a food additive approved by Food and Drug

Administration. CA and its derivatives have been proven effective in boosting H₂O₂ generation, amplifying tumor H₂O₂ levels to increase •OH generation. Numerous strategies based on CA-mediated H₂O₂ generation have

been used to amplify intracellular oxidative stress for triggered the death of cancer cells [77,131–133]. As an example, Kwon et al. skillfully synthesized dual acid-sensitive PolyCAFe micelles, which could concurrently deliver H_2O_2 generator benzoyloxycinnamaldehyde (BCA) and Fenton catalyst Fc into the tumor site, escalating intracellular oxidative stress for preferentially triggered cancer cell death. As shown in Fig. 15, after entering the weakly acidic tumor microenvironment, PolyCAFe micelles would release the BCA and Fc due to the cleavage of the acid-sensitive bond. BCA-mediated H_2O_2 generation could elevate H_2O_2 levels to reinforce Fc-mediated $\bullet\text{OH}$ generation. The *in vitro* and *in vivo* results verified that PolyCAFe micelles existed excellent therapeutic performance and favorable biocompatibility [78]. This study provided an innovative strategy for exploiting new therapeutic nanoplateforms, simultaneously amplifying tumor H_2O_2 levels and enhancing $\bullet\text{OH}$ generation for specifically triggered cancer cell death with remarkable biosafety.

3.6 La-mediated H_2O_2 generation

La as a special H_2O_2 -producing agent could generate $\text{O}_2^{\cdot-}$ and H_2O_2 . After entering cancer cells, La can selectively increase the content of H_2O_2 in tumor sites under the action of overexpressed quinone oxidoreductase 1 (NQO1). La-mediated H_2O_2 generation has been reported and used to improve therapeutical performance in cancers [79–81]. As

a paradigm, Li et al. constructed the self-supply H_2O_2 nanoplatform via loading La into $\text{Fe}@Fe_3\text{O}_4@Cu_{2-x}\text{S}$ -PEG to form $\text{Fe}@Fe_3\text{O}_4@Cu_{2-x}\text{S}@La$ -PEG. As depicted in Fig. 16, La released from $\text{Fe}@Fe_3\text{O}_4@Cu_{2-x}\text{S}@La$ -PEG could selectively boost tumor site-specific H_2O_2 generation under the catalysis of NQO1. Subsequently, the iron and copper ions released from the $\text{Fe}@Fe_3\text{O}_4@Cu_{2-x}\text{S}$ in the acidic environment could convert H_2O_2 into highly toxic $\bullet\text{OH}$ via Fenton reactions, dramatically improving $\bullet\text{OH}$ generation with minimal systemic toxicity due to low NQO1 expression in normal tissues. The *in vivo* results demonstrated that the $\text{Fe}@Fe_3\text{O}_4@Cu_{2-x}\text{S}@La$ -PEG significantly inhibited tumor growth [82]. The therapeutical strategy based on La-mediated H_2O_2 generation provided new insight into the enhancement of tumor-selective $\bullet\text{OH}$ generation, significantly promoting NQO1-overexpressing tumor-cell apoptosis with minimal side effects on normal cells.

4 Conclusions and prospect

The $\bullet\text{OH}$ production is generally considered as H_2O_2 decomposition in the presence of Fenton catalysts via Fenton or Fenton-like reactions. The generated $\bullet\text{OH}$ can induce tumor cell death by attacking and oxidizing intracellular biomolecules, such as DNA, proteins, and polyunsaturated fatty acids. However, the efficacy of $\bullet\text{OH}$ generation is severely hindered by insufficient intracellular

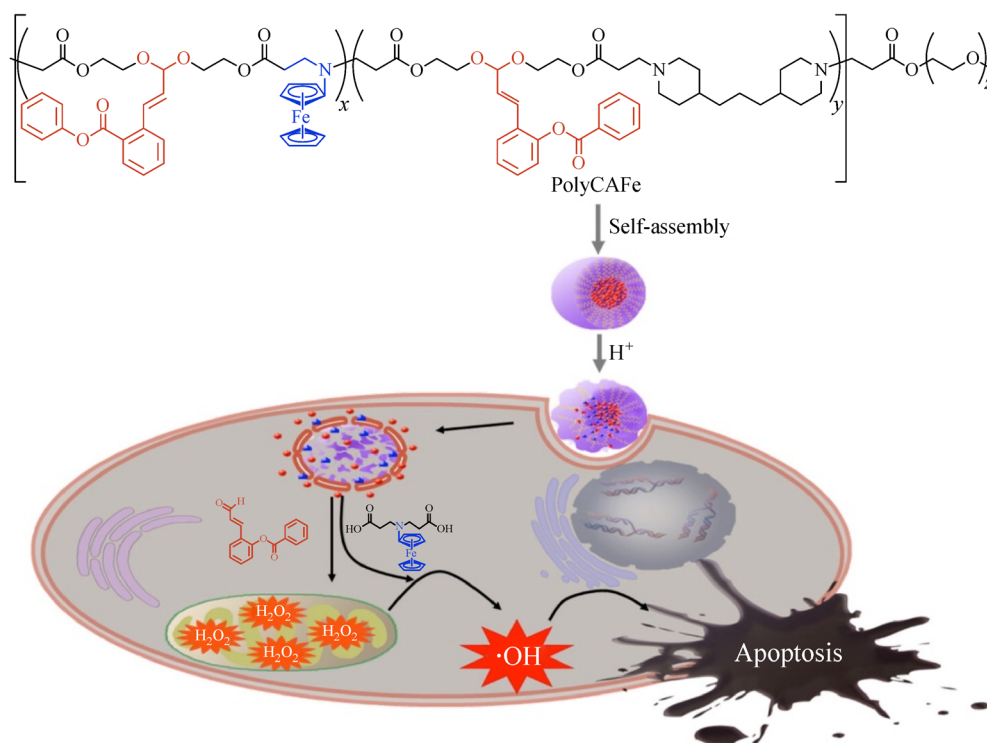


Fig. 15 Schematic diagram of the PolyCAFe-triggered cancer apoptosis via boosting H_2O_2 generation and $\bullet\text{OH}$ generation. Reprinted with permission from ref. [78]. Copyright 2016, American Chemical Society.

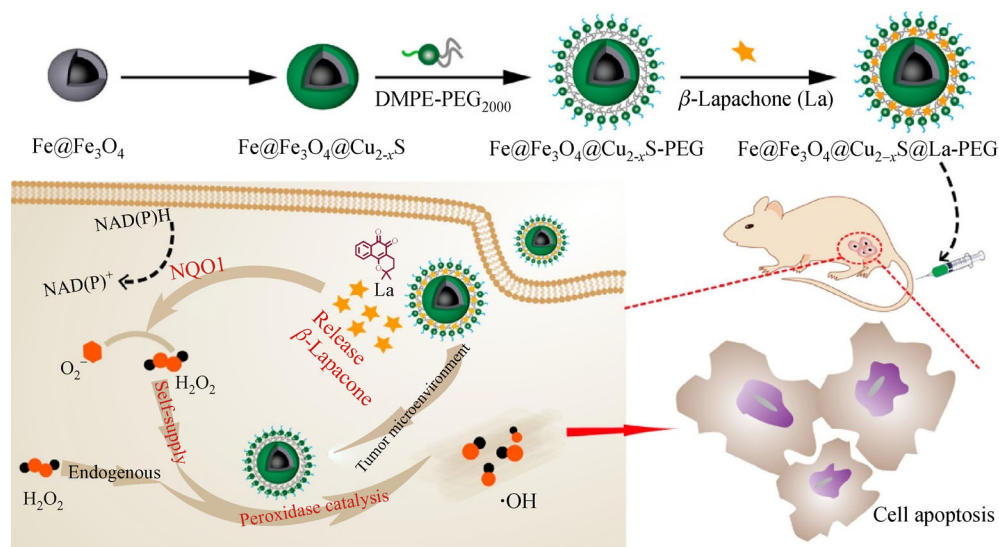


Fig. 16 Illustration of the synthetic process and therapeutic mechanism of $\text{Fe@Fe}_3\text{O}_4\text{@Cu}_{2-x}\text{S@La-PEG}$. Reprinted with permission from ref. [82]. Copyright 2020, American Chemical Society.

H_2O_2 contents and limited Fenton catalysts. Therefore, various strategies have been widely used to improve $\cdot\text{OH}$ generation. This review mainly summarizes current developments of hydroxyl radical-based cancer therapy, including effective supply of typical metal-based Fenton catalysts and up-regulation of H_2O_2 levels in tumor sites. These strategies remarkably enhance the efficacy of $\cdot\text{OH}$ generation, increasing the therapeutic performance.

However, the hydroxyl radical-based cancer therapy still exists the following four problems that need to be further studied and optimized. 1) The excess metal ions introduced into cells can cause severe damages to human health and limit further clinical translation. Therefore, detecting or controlling the amount of metal ion introduction is an effective strategy to avoid damage on normal cells or tissues. 2) The nanocarriers that are used to deliver Fenton catalysts lack tumor-specific target, which may cause damage on normal cells with adverse effects. Consequently, exploiting tumor-target nanocarriers to specifically target tumor cells is an effective strategy to solve this problem. 3) The $\cdot\text{OH}$ generation via the Fenton reaction needs low pH conditions, ranging from 2 to 4. However, the pH of the tumor microenvironment predominantly ranges from 6.5 to 7, the pH of endosomes is approximately 5.0, and the pH of lysosomes is about 4.5. Therefore, decreasing the pH of the tumor microenvironment or delivering nanocarriers to endosomes or lysosomes is an effective approach to enhance the efficiency of $\cdot\text{OH}$ generation. 4) GSH serves as an important antioxidant substance, eliminating the generated ROS to maintain intracellular redox balance. Compared with normal tissues, tumor tissues are mainly characterized by higher GSH content (2 to 10 $\text{mmol}\cdot\text{L}^{-1}$). The therapeutic efficiency of $\cdot\text{OH}$ -based cancer therapy will be limited because of GSH

elimination. Therefore, simultaneously promoting intracellular GSH depletion and increasing ROS generation will enhance the efficiency of $\cdot\text{OH}$ generation. Although there are still some problems required to be further solved and optimized, hydroxyl radical-involved cancer therapy shows high prospect.

Acknowledgements The authors acknowledge the financial support from the Tianjin Science and Technology Committee (Grant No. 19JCYBJC28400), the Basic Research General Program of Shenzhen Science and Technology Innovation Commission in 2020 (Grant No. JCYJ20190806162412752).

References

- Hanahan D, Weinberg R A. Hallmarks of cancer: the next generation. *Cell*, 2011, 144(5): 646–674
- Liou G Y, Storz P. Reactive oxygen species in cancer. *Free Radical Research*, 2010, 44(5): 479–496
- Fridovich I. Superoxide anion radical ($\text{O}_2^{\cdot-}$), superoxide dismutases, and related matters. *Journal of Biological Chemistry*, 1997, 272(30): 18515–18517
- Mi P. Stimuli-responsive nanocarriers for drug delivery, tumor imaging, therapy and theranostics. *Theranostics*, 2020, 10(10): 4557–4588
- Gligorovski S, Strekowski R, Barbati S, Vione D. Environmental implications of hydroxyl radicals ($\cdot\text{OH}$). *Chemical Reviews*, 2015, 115(24): 13051–13092
- Yang B, Ding L, Yao H, Chen Y, Shi J. A metal-organic framework (MOF) Fenton nanoagent-enabled nanocatalytic cancer therapy in synergy with autophagy inhibition. *Advanced Materials*, 2020, 32(12): 1907152–1907164
- Cheng L, Wang C, Feng L, Yang K, Liu Z. Functional

- nanomaterials for phototherapies of cancer. *Chemical Reviews*, 2014, 114(21): 10869–10939
8. Begg A C, Stewart F A, Vens C. Strategies to improve radiotherapy with targeted drugs. *Nature Reviews. Cancer*, 2011, 11(4): 239–253
 9. Pan X, Bai L, Wang H, Wu Q, Wang H, Liu S, Xu B, Shi X, Liu H. Metal-organic-framework-derived carbon nanostructure augmented sonodynamic cancer therapy. *Advanced Materials*, 2018, 30(23): 1800180–1800189
 10. Tang Z, Liu Y, He M, Bu W. Chemodynamic therapy: tumour microenvironment-mediated Fenton and Fenton-like reactions. *Angewandte Chemie International Edition*, 2019, 58(4): 946–956
 11. Kim J, Cho H C, Jeon H, Kim D, Song C, Lee N, Choi S H, Hyeon T. Continuous O₂-evolving MnFe₂O₄ nanoparticle-anchored mesoporous silica nanoparticles for efficient photodynamic therapy in hypoxic cancer. *Journal of the American Chemical Society*, 2017, 139(32): 10992–10995
 12. Wang J, Zhang Y, Archibong E, Ligler F S, Gu Z. Leveraging H₂O₂ levels for biomedical applications. *Advanced Biosystems*, 2017, 1(9): 1700084–1700099
 13. Devine P J, Perreault S D, Luderer U. Roles of reactive oxygen species and antioxidants in ovarian toxicity. *Biology of Reproduction*, 2012, 86(2): 27
 14. Zhang C, Bu W, Ni D, Zhang S, Li Q, Yao Z, Zhang J, Yao H, Wang Z, Shi J. Synthesis of iron nanometallic glasses and their application in cancer therapy by a localized Fenton reaction. *Angewandte Chemie International Edition*, 2016, 55(6): 2101–2106
 15. Liu X, Jin Y, Liu T, Yang S, Zhou M, Wang W, Yu H. Iron-based theranostic nanoplatform for improving chemodynamic therapy of cancer. *ACS Biomaterials Science & Engineering*, 2020, 6(9): 4834–4845
 16. Ranji-Burachaloo H, Gurr P A, Dunstan D E, Qiao G G. Cancer treatment through nanoparticle-facilitated Fenton reaction. *ACS Nano*, 2018, 12(12): 11819–11837
 17. Gao Z, He T, Zhang P, Li X, Zhang Y, Lin J, Hao J, Huang P, Cui J. Polypeptide-based theranostics with tumor-microenvironment-activatable cascade reaction for chemo-ferroptosis combination therapy. *ACS Applied Materials & Interfaces*, 2020, 12(18): 20271–20280
 18. Hentze M W, Muckenthaler M U, Andrews N C. Balancing acts: molecular control of mammalian iron metabolism. *Cell*, 2004, 30(3): 285–297
 19. Dong S, Dong Y, Jia T, Zhang F, Wang Z, Feng L, Sun Q, Gai S, Yang P. Sequential catalytic, magnetic targeting nanoplatform for synergistic photothermal and NIR-enhanced chemodynamic therapy. *Chemistry of Materials*, 2020, 32(23): 9868–9881
 20. Chen G, Yang Y, Xu Q, Ling M, Lin H, Ma M, Sun R, Xu Y, Liu X, Li N, et al. Self-amplification of tumor oxidative stress with degradable metallic complexes for synergistic cascade tumor therapy. *Nano Letters*, 2020, 20(11): 8141–8150
 21. Hou H, Huang X, Wei G, Xu F, Wang Y, Zhou S. Fenton reaction-assisted photodynamic therapy for cancer with multifunctional magnetic nanoparticles. *ACS Applied Materials & Interfaces*, 2019, 11(33): 29579–29592
 22. Zhang Y, Lin L, Liu L, Liu F, Sheng S, Tian H, Chen X. Positive feedback nanoamplifier responded to tumor microenvironments for self-enhanced tumor imaging and therapy. *Biomaterials*, 2019, 216: 119255–119264
 23. Wang D, Wu H, Wang C, Gu L, Chen H, Jana D, Feng L, Liu J, Wang X, Xu P, et al. Self-assembled single-site nanozyme for tumor-specific amplified cascade enzymatic therapy. *Angewandte Chemie International Edition*, 2021, 60(6): 3001–3007
 24. Liu X, Jin Y, Liu T, Yang S, Zhou M, Wang W, Yu H. Iron-based theranostic nanoplatform for improving chemodynamic therapy of cancer. *ACS Biomaterials Science & Engineering*, 2020, 6(9): 4834–4845
 25. Jiang F, Ding B, Liang S, Zhao Y, Cheng Z, Xing B, Ma P, Lin J. Intelligent MoS₂-CuO heterostructures with multiplexed imaging and remarkably enhanced antitumor efficacy via synergetic photothermal therapy/chemodynamic therapy/immunotherapy. *Biomaterials*, 2021, 268: 120545–120557
 26. Cao S, Fan J, Sun W, Li F, Li K, Tai X, Peng X. A novel Mn-Cu bimetallic complex for enhanced chemodynamic therapy with simultaneous glutathione depletion. *Chemical Communications*, 2019, 55(86): 12956–12959
 27. Wang C, Yang J, Dong C, Shi S. Glucose oxidase-related cancer therapies. *Advanced Therapeutics*, 2020, 3(10): 2000110–2000139
 28. Lou-Franco J, Das B, Elliott C, Cao C. Gold nanozymes: from concept to biomedical applications. *Nano-Micro Letters*, 2021, 13(1): 10–46
 29. Chen Y, Deng J, Liu F, Dai P, An Y, Wang Z, Zhao Y. Energy-free, singlet oxygen-based chemodynamic therapy for selective tumor treatment without dark toxicity. *Advanced Healthcare Materials*, 2019, 8(18): 1900366–1900376
 30. Sullivan L B, Chandel N S. Mitochondrial reactive oxygen species and cancer. *Cancer & Metabolism*, 2014, 2(1): 17–29
 31. Hu H, Yu L, Qian X, Chen Y, Chen B, Li Y. Chemoreactive nanotherapeutics by metal peroxide based nanomedicine. *Advancement of Science*, 2020, 8(1): 2000494–2000511
 32. Ka H, Park H J, Jung H J, Choi J W, Cho K S, Ha J, Lee K T. Cinnamaldehyde induces apoptosis by ROS-mediated mitochondrial permeability transition in human promyelocytic leukemia HL-60 cells. *Cancer Letters*, 2003, 196(2): 143–152
 33. Ahn K J, Lee H S, Bai S K, Song C W. Enhancement of radiation effect using beta-lapachone and underlying mechanism. *Radiation Oncology Journal*, 2013, 31(2): 57–65
 34. Huang C, Liao Z, Lu H, Pan W, Wan W, Chen C, Sung H. Cellular organelle-dependent cytotoxicity of iron oxide nanoparticles and its implications for cancer diagnosis and treatment: a mechanistic investigation. *Chemistry of Materials*, 2016, 28(24): 9017–9025
 35. Zhang Y, Wan Y, Liao Y, Hu Y, Jiang T, He T, Bi W, Lin J, Gong P, Tang L, et al. Janus γ -Fe₂O₃/SiO₂-based nanotheranostics for dual-modal imaging and enhanced synergistic cancer starvation/chemodynamic therapy. *Science Bulletin*, 2020, 65(7): 564–572
 36. Liu Z, Li T, Han F, Wang Y, Gan Y, Shi J, Wang T, Akhtar M L, Li Y. A cascade-reaction enabled synergistic cancer starvation/ROS-mediated/chemo-therapy with an enzyme modified Fe-based MOF. *Biomaterials Science*, 2019, 7(9): 3683–3692
 37. Wang L, Huo M, Chen Y, Shi J. Iron-engineered mesoporous silica nanocatalyst with biodegradable and catalytic framework for tumor-specific therapy. *Biomaterials*, 2018, 163: 1–13

38. He T, Yuan Y, Jiang C, Blum N T, He J, Huang P, Lin J. Light-triggered transformable ferrous ion delivery system for photo-thermal primed chemodynamic therapy. *Angewandte Chemie International Edition*, 2021, 60(11): 6047–6054
39. Yu J, Zhao F, Gao W, Yang X, Ju Y, Zhao L, Guo W, Xie J, Liang X, Tao X, et al. Magnetic reactive oxygen species nanoreactor for switchable magnetic resonance imaging guided cancer therapy based on pH-sensitive $\text{Fe}_3\text{C}_2@\text{Fe}_3\text{O}_4$ nanoparticles. *ACS Nano*, 2019, 13(9): 10002–10014
40. Yao Z, Zhang B, Liang T, Ding J, Min Q, Zhu J. Promoting oxidative stress in cancer starvation therapy by site-specific startup of hyaluronic acid-enveloped dual-catalytic nanoreactors. *ACS Applied Materials & Interfaces*, 2019, 11(21): 18995–19005
41. Gao F, Wang F, Nie X, Zhang Z, Chen G, Xia L, Wang L, Wang C, Hao Z, Zhang W, et al. Mitochondria-targeted delivery and light controlled release of iron prodrug and CO to enhance cancer therapy by ferroptosis. *New Journal of Chemistry*, 2020, 44(8): 3478–3486
42. Nie X, Xia L, Wang H, Chen G, Wu B, Zeng T, Hong C, Wang L, You Y. Photothermal therapy nanomaterials boosting transformation of Fe(III) into Fe(II) in tumor cells for highly improving chemodynamic therapy. *ACS Applied Materials & Interfaces*, 2019, 11(35): 31735–31742
43. Fang C, Deng Z, Cao G, Chu Q, Wu Y, Li X, Peng X, Han G. Co-ferrocene MOF/glucose oxidase as cascade nanozyme for effective tumor therapy. *Advanced Functional Materials*, 2020, 30(16): 1910085–1910094
44. Deng Z, Fang C, Ma X, Li X, Zeng Y J, Peng X. One stone two birds: Zr-Fc metal-organic framework nanosheet for synergistic photothermal and chemodynamic cancer therapy. *ACS Applied Materials & Interfaces*, 2020, 12(18): 20321–20330
45. Na Y, Woo J, Choi W I, Sung D. Novel carboxylated ferrocene polymer nanocapsule with high reactive oxygen species sensitivity and on-demand drug release for effective cancer therapy. *Colloids and Surfaces. B, Biointerfaces*, 2021, 200: 111566–111572
46. Chen Y, Yao Y, Zhou X, Liao C, Dai X, Liu J, Yu Y, Zhang S. Cascade-reaction-based nanodrug for combined chemo/starvation/chemodynamic therapy against multidrug-resistant tumors. *ACS Applied Materials & Interfaces*, 2019, 11(49): 46112–46123
47. Zhang L, Wan S, Li C, Xu L, Cheng H, Zhang X. An adenosine triphosphate-responsive autocatalytic Fenton nanoparticle for tumor ablation with self-supplied H_2O_2 and acceleration of Fe (III)/Fe(II) conversion. *Nano Letters*, 2018, 18(12): 7609–7618
48. Dong Z, Feng L, Chao Y, Hao Y, Chen M, Gong F, Han X, Zhang R, Cheng L, Liu Z. Amplification of tumor oxidative stresses with liposomal Fenton catalyst and glutathione inhibitor for enhanced cancer chemotherapy and radiotherapy. *Nano Letters*, 2019, 19(2): 805–815
49. Liu T, Liu W, Zhang M, Yu W, Gao F, Li C, Wang S, Feng J, Zhang X. Ferrous-supply-regeneration nanoengineering for cancer-cell-specific ferroptosis in combination with imaging-guided photodynamic therapy. *ACS Nano*, 2018, 12(12): 12181–12192
50. Shan L, Gao G, Wang W, Tang W, Wang Z, Yang Z, Fan W, Zhu G, Zhai K, Jacobson O, et al. Self-assembled green tea polyphenol-based coordination nanomaterials to improve chemotherapy efficacy by inhibition of carbonyl reductase 1. *Biomaterials*, 2019, 210: 62–69
51. Mu M, Wang Y, Zhao S, Li X, Fan R, Mei L, Wu M, Zou B, Zhao N, Han B, Guo G. Engineering a pH/glutathione-responsive tea polyphenol nanodevice as an apoptosis/ferroptosis-inducing agent. *ACS Applied Bio Materials*, 2020, 3(7): 4128–4138
52. He T, Qin X, Jiang C, Jiang D, Lei S, Lin J, Zhu W G, Qu J, Huang P. Tumor pH-responsive metastable-phase manganese sulfide nanotheranostics for traceable hydrogen sulfide gas therapy primed chemodynamic therapy. *Theranostics*, 2020, 10(6): 2453–2462
53. Fu L H, Hu Y R, Qi C, He T, Jiang S, Jiang C, He J, Qu J, Lin J, Huang P. Biodegradable manganese-doped calcium phosphate nanotheranostics for traceable cascade reaction-enhanced anti-tumor therapy. *ACS Nano*, 2019, 13(12): 13985–13994
54. He T, Jiang C, He J, Zhang Y, He G, Wu J, Lin J, Zhou X, Huang P. Manganese-dioxide-coating-instructed plasmonic modulation of gold nanorods for activatable duplex-imaging-guided NIR-II photothermal-chemodynamic therapy. *Advanced Materials*, 2021, 33(13): 2008540–2008550
55. Qi C, He J, Fu L H, He T, Blum N T, Yao X, Lin J, Huang P. Tumor-specific activatable nanocarriers with gas-generation and signal amplification capabilities for tumor theranostics. *ACS Nano*, 2021, 15(1): 1627–1639
56. Fu L H, Wan Y, Li C, Qi C, He T, Yang C, Zhang Y, Lin J, Huang P. Biodegradable calcium phosphate nanotheranostics with tumor-specific activatable cascade catalytic reactions-augmented photodynamic therapy. *Advanced Functional Materials*, 2021, 31(14): 2009848–2009859
57. Lin L S, Song J, Song L, Ke K, Liu Y, Zhou Z, Shen Z, Li J, Yang Z, Tang W, et al. Simultaneous Fenton-like ion delivery and glutathione depletion by MnO_2 -based nanoagent to enhance chemodynamic therapy. *Angewandte Chemie International Edition*, 2018, 57(18): 4902–4906
58. Wang Z, Liu B, Sun Q, Dong S, Kuang Y, Dong Y, He F, Gai S, Yang P. Fusiform-like copper(II)-based metal-organic framework through relief hypoxia and GSH-depletion Co-enhanced starvation and chemodynamic synergistic cancer therapy. *ACS Applied Materials & Interfaces*, 2020, 12(15): 17254–17267
59. Hu R, Fang Y, Huo M, Ya H, Wang C, Chen Y, Wu R. Ultrasmall Cu_{2-x}S nanodots as photothermal-enhanced Fenton nanocatalysts for synergistic tumor therapy at NIR-II biowindow. *Biomaterials*, 2019, 206: 101–114
60. Wang X, Zhong X, Lei H, Geng Y, Zhao Q, Gong F, Yang Z, Dong Z, Liu Z, Cheng L. Hollow Cu_2Se nanozymes for tumor photothermal-catalytic therapy. *Chemistry of Materials*, 2019, 31(16): 6174–6186
61. Fu L H, Wan Y, Qi C, He J, Li C, Yang C, Xu H, Lin J, Huang P. Nanocatalytic theranostics with glutathione depletion and enhanced reactive oxygen species generation for efficient cancer therapy. *Advanced Materials*, 2021, 33(7): 2006892–2006903
62. Yang C, Younis M R, Zhang J, Qu J, Lin J, Huang P. Programmable NIR-II photothermal-enhanced starvation-primed chemodynamic therapy using glucose oxidase-functionalized ancient pigment nanosheets. *Small*, 2020, 16(25): 2001518–2001528
63. Ma B, Wang S, Liu F, Zhang S, Duan J, Li Z, Kong Y, Sang Y, Liu H, Bu W, et al. Self-assembled copper-amino acid nanoparticles

- for *in situ* glutathione “and” H₂O₂ sequentially triggered chemodynamic therapy. *Journal of the American Chemical Society*, 2019, 141(2): 849–857
64. Huo M, Wang L, Chen Y, Shi J. Tumor-selective catalytic nanomedicine by nanocatalyst delivery. *Nature Communications*, 2017, 8(1): 357–369
 65. He T, Xu H, Zhang Y, Yi S, Cui R, Xing S, Wei C, Lin J, Huang P. Glucose oxidase-instructed traceable self-oxygenation/hyperthermia dually enhanced cancer starvation therapy. *Theranostics*, 2020, 10(4): 1544–1554
 66. Feng L, Xie R, Wang C, Gai S, He F, Yang D, Yang P, Lin J. Magnetic targeting, tumor microenvironment responsive intelligent nanocatalysts for enhanced tumor ablation. *ACS Nano*, 2018, 12(11): 11000–11012
 67. Ding Y, Xu H, Xu C, Tong Z, Zhang S, Bai Y, Chen Y, Xu Q, Zhou L, Ding H, et al. A nanomedicine fabricated from gold nanoparticles-decorated metal-organic framework for cascade chemo/chemodynamic cancer therapy. *Advancement of Science*, 2020, 7(17): 2001060–2001070
 68. Gao S, Lin H, Zhang H, Yao H, Chen Y, Shi J. Nanocatalytic tumor therapy by biomimetic dual inorganic nanozyme-catalyzed cascade reaction. *Advancement of Science*, 2019, 6(3): 1801733–1801745
 69. Ma P, Xiao H, Yu C, Liu J, Cheng Z, Song H, Zhang X, Li C, Wang J, Gu Z, et al. Enhanced cisplatin chemotherapy by iron oxide nanocarrier-mediated generation of highly toxic reactive oxygen species. *Nano Letters*, 2017, 17(2): 928–937
 70. Sang Y, Cao F, Li W, Zhang L, You Y, Deng Q, Dong K, Ren J, Qu X. Bioinspired construction of a nanozyme-based H₂O₂ homeostasis disruptor for intensive chemodynamic therapy. *Journal of the American Chemical Society*, 2020, 142(11): 5177–5183
 71. Wang Y, Yin W, Ke W, Chen W, He C, Ge Z. Multifunctional polymeric micelles with amplified Fenton reaction for tumor ablation. *Biomacromolecules*, 2018, 19(6): 1990–1998
 72. An Y, Zhu J, Liu F, Deng J, Meng X, Liu G, Wu H, Fan A, Wang Z, Zhao Y. Boosting the ferroptotic antitumor efficacy via site-specific amplification of tailored lipid peroxidation. *ACS Applied Materials & Interfaces*, 2019, 11(33): 29655–29666
 73. Han Y, Ouyang J, Li Y, Wang F, Jiang J H. Engineering H₂O₂ self-supplying nanotheranostic platform for targeted and imaging-guided chemodynamic therapy. *ACS Applied Materials & Interfaces*, 2020, 12(1): 288–297
 74. Gao S, Lu X, Zhu P, Lin H, Yu L, Yao H, Wei C, Chen Y, Shi J. Self-evolved hydrogen peroxide boosts photothermal-promoted tumor-specific nanocatalytic therapy. *Journal of Materials Chemistry. B, Materials for Biology and Medicine*, 2019, 7(22): 3599–3609
 75. Lin L, Huang T, Song J, Ou X, Wang Z, Deng H, Tian R, Liu Y, Wang J, Liu Y, et al. Synthesis of copper peroxide nanodots for H₂O₂ self-supplying chemodynamic therapy. *Journal of the American Chemical Society*, 2019, 141(25): 9937–9945
 76. Zhang S, Cao C, Lv X, Dai H, Zhong Z, Liang C, Wang W, Huang W, Song X, Dong X A. H₂O₂ self-sufficient nanoplatform with domino effects for thermal-responsive enhanced chemodynamic therapy. *Chemical Science (Cambridge)*, 2020, 11(7): 1926–1934
 77. Xu X, Zeng Z, Chen J, Huang B, Guan Z, Huang Y, Huang Z, Zhao C. Tumor-targeted supramolecular catalytic nanoreactor for synergistic chemo/chemodynamic therapy via oxidative stress amplification and cascaded Fenton reaction. *Chemical Engineering Journal*, 2020, 390: 124628–124644
 78. Kwon B, Han E, Yang W, Cho W, Yoo W, Hwang J, Kwon B M, Lee D. Nano-Fenton reactors as a new class of oxidative stress amplifying anticancer therapeutic agents. *ACS Applied Materials & Interfaces*, 2016, 8(9): 5887–5897
 79. Wang S, Wang Z, Yu G, Zhou Z, Jacobson O, Liu Y, Ma Y, Zhang F, Chen Z Y, Chen X. Tumor-specific drug release and reactive oxygen species generation for cancer chemo/chemodynamic combination therapy. *Advancement of Science*, 2019, 6(5): 1801986–1801993
 80. Wang S, Yu G, Wang Z, Jacobson O, Lin L S, Yang W, Deng H, He Z, Liu Y, Chen Z Y, et al. Enhanced antitumor efficacy by a cascade of reactive oxygen species generation and drug release. *Angewandte Chemie International Edition*, 2019, 58(41): 14758–14763
 81. Chen Q, Zhou J, Chen Z, Luo Q, Xu J, Song G. Tumor-specific expansion of oxidative stress by glutathione depletion and use of a Fenton nanoagent for enhanced chemodynamic therapy. *ACS Applied Materials & Interfaces*, 2019, 11(34): 30551–30565
 82. Li X, Zhao C, Deng G, Liu W, Shao J, Zhou Z, Liu F, Yang H, Yang S. Nanozyme-augmented tumor catalytic therapy by self-supplied H₂O₂ generation. *ACS Applied Bio Materials*, 2020, 3(3): 1769–1778
 83. Attia M F, Anton N, Wallyn J, Omran Z, Vandamme T F. An overview of active and passive targeting strategies to improve the nanocarriers efficiency to tumour sites. *Journal of Pharmacy and Pharmacology*, 2019, 71(8): 1185–1198
 84. Din F U, Aman W, Ullah I, Qureshi O S, Mustapha O, Shafique S, Zeb A. Effective use of nanocarriers as drug delivery systems for the treatment of selected tumors. *International Journal of Nanomedicine*, 2017, 12: 7291–7309
 85. Khodabandehloo H, Zahednasab H, Hafez A A. Nanocarriers usage for drug delivery in cancer therapy. *Iranian Journal of Cancer Prevention*, 2016, 9(2): 3966–3973
 86. Sutrisno L, Hu Y, Hou Y, Cai K, Li M, Luo Z. Progress of iron-based nanozymes for antitumor therapy. *Frontiers in Chemistry*, 2020, 8: 680–689
 87. Hagen H, Marzenell P, Jentzsch E, Wenz F, Veldwijk M R, Mokhir A. Aminoferrocene-based prodrugs activated by reactive oxygen species. *Journal of Medicinal Chemistry*, 2012, 55(2): 924–934
 88. Hu M, Ju Y, Liang K, Suma T, Cui J, Caruso F. Void engineering in metal-organic frameworks via synergistic etching and surface functionalization. *Advanced Functional Materials*, 2016, 26(32): 5827–5834
 89. Yang W, Sousa A M M, Thomas-Gahring A, Fan X, Jin T, Li X, Tomasula P M, Liu L. Electrospun polymer nanofibers reinforced by tannic acid/Fe⁺⁺⁺ complex. *Materials (Basel)*, 2016, 9(9): 757–769
 90. Lu S C. Regulation of glutathione synthesis. *Molecular Aspects of Medicine*, 2009, 30(1-2): 42–59
 91. Wan S S, Cheng Q, Zeng X, Zhang X Z A. Mn(III)-sealed metal-organic-framework nanosystem for redox-unlocked tumor theranostics. *ACS Nano*, 2019, 13(6): 6561–6571

92. Zhao H, Wang Y, Wang Y, Cao T, Zhao G. Electro-Fenton oxidation of pesticides with a novel $\text{Fe}_3\text{O}_4@/\text{Fe}_2\text{O}_3$ /activated carbon aerogel cathode: high activity, wide pH range and catalytic mechanism. *Applied Catalysis B: Environmental*, 2012, 125: 120–127
93. Masomboon N, Ratanatamskul C, Lu M C. Chemical oxidation of 2, 6-dimethylaniline in the Fenton process. *Environmental Science & Technology*, 2009, 43(22): 8629–8634
94. Brillas E, Banos M A, Camps S, Arias C, Cabot P L, Garrido J A, Rodriguez R M. Catalytic effect of Fe^{2+} , Cu^{2+} and UVA light on the electrochemical degradation of nitrobenzene using an oxygen-diffusion cathode. *New Journal of Chemistry*, 2004, 28(2): 314–322
95. Li T, Zhou J, Wang L, Zhang H, Song C, Fuente J M, Pan Y, Song J, Zhang C, Cui D. Photo-Fenton-like metal-protein self-assemblies as multifunctional tumor theranostic agent. *Advanced Healthcare Materials*, 2019, 8(15): 1900192–1900204
96. Zhang W, Lu J, Gao X, Li P, Zhang W, Ma Y, Wang H, Tang B. Enhanced photodynamic therapy by reduced levels of intracellular glutathione obtained by employing a nano-MOF with Cu(II) as the active center. *Angewandte Chemie International Edition*, 2018, 57(18): 4891–4896
97. Fu L H, Qi C, Hu Y R, Lin J, Huang P. Glucose oxidase-instructed multimodal synergistic cancer therapy. *Advanced Materials*, 2019, 31(21): 1808325–1808339
98. Zheng X, Liu Q, Jing C, Li Y, Li D, Luo W, Wen Y, He Y, Huang Q, Long Y T, et al. Catalytic gold nanoparticles for nanoplasmonic detection of DNA hybridization. *Angewandte Chemie International Edition*, 2011, 50(50): 12200–12204
99. Zhang J, Mou L, Jiang X. Surface chemistry of gold nanoparticles for health-related applications. *Chemical Science (Cambridge)*, 2020, 11(4): 923–936
100. Ighodaro O M, Akinloye O A. First line defence antioxidants-superoxide dismutase (SOD), catalase (CAT) and glutathione peroxidase (GPX): their fundamental role in the entire antioxidant defence grid. *Alexandria Journal of Medicine*, 2018, 54(4): 287–293
101. Singh S. Nanomaterials exhibiting enzyme-like properties (nanozymes): current advances and future perspectives. *Frontiers in Chemistry*, 2019, 7: 46–56
102. Kim Y S, Vallur P G, Phaëton R, Mythreye K, Hempel N. Insights into the dichotomous regulation of SOD2 in cancer. *Antioxidants*, 2017, 6(4): 86–111
103. Wang X, Chen N, Liu X, Shi Y, Ling C, Zhang L. Ascorbate guided conversion of hydrogen peroxide to hydroxyl radical on goethite. *Applied Catalysis B: Environmental*, 2021, 282: 119558–119565
104. Gao S, Jin Y, Ge K, Li Z, Liu H, Dai X, Zhang Y, Chen S, Liang X, Zhang J. Self-supply of O_2 and H_2O_2 by a nanocatalytic medicine to enhance combined chemo/chemodynamic therapy. *Advancement of Science*, 2019, 6(24): 1902137–1902146
105. He C, Zhang X, Xiang G. Nanoparticle facilitated delivery of peroxides for effective cancer treatments. *Biomaterials Science*, 2020, 8(20): 5574–5582
106. Golikova E P, Lakina N V, Grebennikova O V, Matveeva V G, Sulman E M. A study of biocatalysts based on glucose oxidase. *Faraday Discussions*, 2017, 202: 303–314
107. Bankar S B, Bule M V, Singhal R S, Ananthanarayan L. Glucose oxidase—an overview. *Biotechnology Advances*, 2009, 27(4): 489–501
108. Zhao L, Wang L, Zhang Y, Xiao S, Bi F, Zhao J, Gai G, Ding J. Glucose oxidase-based glucose-sensitive drug delivery for diabetes treatment. *Polymers*, 2017, 9(7): 255–276
109. Karunwi O, Guiseppi-Elie A. Supramolecular glucose oxidase-SWNT conjugates formed by ultrasonication: effect of tube length, functionalization and processing time. *Journal of Nanobiotechnology*, 2013, 11(1): 6–22
110. Zeng L, Huang K, Wan Y, Zhang J, Yao X, Jiang C, Lin J, Huang P. Programmable starving-photodynamic synergistic cancer therapy. *Science China Materials*, 2020, 63(4): 611–619
111. Zhang Y, Yang Y, Jiang S, Li F, Lin J, Wang T, Huang P. Degradable silver-based nanoplatfor for synergistic cancer starving-like/metal ion therapy. *Materials Horizons*, 2019, 6(1): 169–175
112. Fu L H, Qi C, Lin J, Huang P. Catalytic chemistry of glucose oxidase in cancer diagnosis and treatment. *Chemical Society Reviews*, 2018, 47(17): 6454–6472
113. Fan W, Lu N, Huang P, Liu Y, Yang Z, Wang S, Yu G, Liu Y, Hu J, He Q, et al. Glucose-responsive sequential generation of hydrogen peroxide and nitric oxide for synergistic cancer starving-like/gas therapy. *Angewandte Chemie International Edition*, 2017, 56(5): 1229–1233
114. Comotti M, Pina C D, Matarrese R, Rossi M. The catalytic activity of “naked” gold particles. *Angewandte Chemie International Edition*, 2004, 43(43): 5812–5815
115. Comotti M, Pina C D, Falletta E, Rossi M. Aerobic oxidation of glucose with gold catalyst: hydrogen peroxide as intermediate and reagent. *Advanced Synthesis & Catalysis*, 2006, 348(3): 313–316
116. Mu J, He L, Fan W, Tang W, Wang Z, Jiang C, Zhang D, Liu Y, Deng H, Zou J, et al. Cascade reactions catalyzed by planar metal-organic framework hybrid architecture for combined cancer therapy. *Small*, 2020, 16(42): 2004016–2004024
117. Jiang D, Ni D, Rosenkrans Z T, Huang P, Yan X, Cai W. Nanozyme: new horizons for responsive biomedical applications. *Chemical Society Reviews*, 2019, 48(14): 3683–3704
118. Malik A, Sultana M, Qazi A, Qazi M H, Parveen G, Waqar S, Ashraf A B, Rasool M. Role of natural radiosensitizers and cancer cell radioresistance: an update. *Analytical Cellular Pathology*, 2016, 2016: 2016–2021
119. Nedeljkovic Z S, Gokce N, Loscalzo J. Mechanisms of oxidative stress and vascular dysfunction. *Postgraduate Medical Journal*, 2003, 79(930): 195–200
120. Pandey K B, Rizvi S I. Markers of oxidative stress in erythrocytes and plasma during aging in humans. *Oxidative Medicine and Cellular Longevity*, 2010, 3(1): 2–12
121. Ohno S, Ohno Y, Suzuki N, Soma G I, Inoue M. High-dose vitamin C (ascorbic acid) therapy in the treatment of patients with advanced cancer. *Anticancer Research*, 2009, 29(3): 809–815
122. Chen Q, Espey M G, Sun A Y, Lee J H, Krishna M C, Shacter E, Choyke P L, Pooput C, Kirk K L, Buettner G R, et al. Ascorbate in pharmacologic concentrations selectively generates ascorbate radical and hydrogen peroxide in extracellular fluid *in vivo*.

- Proceedings of the National Academy of Sciences of the United States of America, 2007, 104(21): 8749–8754
123. Chen Q, Espey M G, Krishna M C, Mitchell J B, Corpe C P, Buettner G R, Shacter E, Levine M. Pharmacologic ascorbic acid concentrations selectively kill cancer cells: action as a pro-drug to deliver hydrogen peroxide to tissues. Proceedings of the National Academy of Sciences of the United States of America, 2005, 102(38): 13604–13609
124. Chen Q, Espey M G, Sun A Y, Pooput C, Kirk K L, Krishna M C, Khosh D B, Drisko J, Levine M. Pharmacologic doses of ascorbate act as a prooxidant and decrease growth of aggressive tumor xenografts in mice. Proceedings of the National Academy of Sciences of the United States of America, 2008, 105(32): 11105–11109
125. Ma Y, Chapman J, Levine M, Polireddy K, Drisko J, Chen Q. High-dose parenteral ascorbate enhanced chemosensitivity of ovarian cancer and reduced toxicity of chemotherapy. Science Translational Medicine, 2014, 6(222): 222ra18
126. Yun J, Mullarky E, Lu C, Bosch K N, Kavalier A, Rivera K, Roper J, Chio I I C, Giannopoulou E G, Rago C, et al. Vitamin C selectively kills KRAS and BRAF mutant colorectal cancer cells by targeting GAPDH. Science, 2015, 350(6266): 1391–1396
127. Li X, Du Y, Wang H, Ma H, Wu D, Ren X, Wei Q, Xu J J. Self-supply of H₂O₂ and O₂ by hydrolyzing CaO₂ to enhance the electrochemiluminescence of luminol based on a closed bipolar electrode. Analytical Chemistry, 2020, 92(18): 12693–12699
128. Huang C C, Chia W T, Chung M F, Lin K J, Hsiao C W, Jin C, Lim W H, Chen C C, Sung H W. An implantable depot that can generate oxygen *in situ* for overcoming hypoxia-induced resistance to anticancer drugs in chemotherapy. Journal of the American Chemical Society, 2016, 138(16): 5222–5225
129. Lin L S, Wang J F, Song J, Liu Y, Zhu G, Dai Y, Shen Z, Tian R, Song J, Wang Z, et al. Cooperation of endogenous and exogenous reactive oxygen species induced by zinc peroxide nanoparticles to enhance oxidative stress-based cancer therapy. Theranostics, 2019, 9(24): 7200–7209
130. Yan Z, Bing W, Ding C, Dong K, Ren J, Qu X A. H₂O₂-free depot for treating bacterial infection: localized cascade reactions to eradicate biofilms *in vivo*. Nanoscale, 2018, 10(37): 17656–17662
131. Kim B, Lee E, Kim Y, Park S, Khang G, Lee D. Dual acid-responsive micelle-forming anticancer polymers as new anticancer therapeutics. Advanced Functional Materials, 2013, 23(40): 5091–5097
132. Noh J, Kwon B, Han E, Park M, Yang W, Cho W, Yoo W, Khang G, Lee D. Amplification of oxidative stress by a dual stimuli-responsive hybrid drug enhances cancer cell death. Nature Communications, 2015, 20(6): 6907–6916
133. Cionti C, Taroni T, Sabatini V, Meroni D. Nanostructured oxide-based systems for the pH-triggered release of cinnamaldehyde. Materials (Basel), 2021, 14(6): 1536–1548